

Review

# Recent Developments in Carbon-11 Chemistry and Applications for First-In-Human PET Studies

Anna Pees<sup>1</sup>, Melissa Chassé<sup>1,2</sup>, Anton Lindberg<sup>1</sup> and Neil Vasdev<sup>1,2,3,\*</sup> 

<sup>1</sup> Azrieli Centre for Neuro-Radiochemistry, Brain Health Imaging Centre, Centre for Addiction and Mental Health (CAMH), Toronto, ON M5T 1R8, Canada

<sup>2</sup> Institute of Medical Science, University of Toronto, Toronto, ON M5S 1A8, Canada

<sup>3</sup> Department of Psychiatry, University of Toronto, Toronto, ON M5T 1R8, Canada

\* Correspondence: neil.vasdev@utoronto.ca

**Abstract:** Positron emission tomography (PET) is a molecular imaging technique that makes use of radiolabelled molecules for in vivo evaluation. Carbon-11 is a frequently used radionuclide for the labelling of small molecule PET tracers and can be incorporated into organic molecules without changing their physicochemical properties. While the short half-life of carbon-11 ( $^{11}\text{C}$ ;  $t_{1/2} = 20.4$  min) offers other advantages for imaging including multiple PET scans in the same subject on the same day, its use is limited to facilities that have an on-site cyclotron, and the radiochemical transformations are consequently more restrictive. Many researchers have embraced this challenge by discovering novel carbon-11 radiolabelling methodologies to broaden the synthetic versatility of this radionuclide. This review presents new carbon-11 building blocks and radiochemical transformations as well as PET tracers that have advanced to first-in-human studies over the past five years.

**Keywords:** Carbon-11; positron emission tomography (PET); radiochemistry; radiotracer; first-in-human



**Citation:** Pees, A.; Chassé, M.; Lindberg, A.; Vasdev, N. Recent Developments in Carbon-11 Chemistry and Applications for First-In-Human PET Studies. *Molecules* **2023**, *28*, 931. <https://doi.org/10.3390/molecules28030931>

Academic Editor: Svend Borup Jensen

Received: 2 December 2022

Revised: 9 January 2023

Accepted: 10 January 2023

Published: 17 January 2023



**Copyright:** © 2023 by the authors. Licensee MDPI, Basel, Switzerland. This article is an open access article distributed under the terms and conditions of the Creative Commons Attribution (CC BY) license (<https://creativecommons.org/licenses/by/4.0/>).

## 1. Introduction

Positron emission tomography (PET) is a molecular imaging technique that utilizes radiotracers for in vivo studies. The radionuclides fluorine-18 and carbon-11 are the most commonly used for labelling PET tracers because of the growing use of organofluorine drugs and as carbon is ubiquitous in nearly every drug or biomolecule. Additionally, their suitable decay characteristics and half-lives match the in vivo pharmacokinetics of small molecules. Consequently, developing new radiochemistry methods for the introduction of these short-lived radionuclides into organic molecules has emerged as one of the greatest challenges in PET radiopharmaceutical chemistry. Our ultimate goal is to radiolabel any molecule for medical imaging—a concept analogous to total synthesis that we introduced as “total radiosynthesis” [1]. Because the radiochemistry of fluorine-18 has been extensively reviewed in recent years [for example see: [2–11]], the focus of this review is on recent radiochemistry methodologies with carbon-11 and translation of  $^{11}\text{C}$ -labelled PET tracers to first-in-human (FIH) PET imaging studies.

Carbon-11 ( $^{11}\text{C}$ ) has a half-life of 20.4 min and is produced in a cyclotron by proton bombardment of nitrogen gas in presence of trace amounts of oxygen (0.1–2%) or hydrogen (5–10%) where it is obtained as  $[^{11}\text{C}]\text{CO}_2$  or  $[^{11}\text{C}]\text{CH}_4$ , respectively [12,13].  $[^{11}\text{C}]\text{CO}_2$  and  $[^{11}\text{C}]\text{CH}_4$  can either be used directly in radiolabelling reactions or further converted to other  $^{11}\text{C}$ -building blocks (see Scheme 1) [14]. The most common carbon-11 labelling strategy for PET tracers is  $^{11}\text{C}$ -methylation of hydroxy or amino groups using  $[^{11}\text{C}]\text{methyl iodide}$  or  $[^{11}\text{C}]\text{methyl triflate}$ , which are routinely obtained from  $[^{11}\text{C}]\text{CO}_2$  and/or  $[^{11}\text{C}]\text{CH}_4$ . The advantages of  $^{11}\text{C}$ -methylation are the accessibility of precursors and carbon-11 methylating agents, as well as the general prevalence of methyl groups in pharmaceutical compounds. However, amongst molecules targeting the central nervous system (CNS) the prevalence of

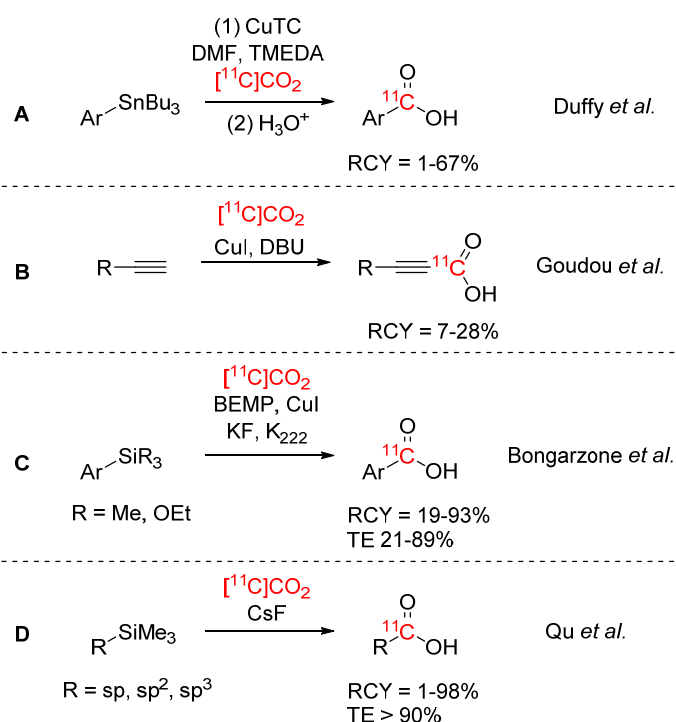


While  $[^{11}\text{C}]\text{CO}_2$  is directly produced in the cyclotron, the irradiated cyclotron target gas contains many undesired chemical and radiochemical entities. To purify  $[^{11}\text{C}]\text{CO}_2$  from carrier gases and other by-products, it is typically trapped using liquid nitrogen or by physical adsorption on porous polymers, such as carbon molecular sieves or polydivinylbenzene copolymers. A new method for purifying  $[^{11}\text{C}]\text{CO}_2$ , also inspired by green chemistry literature, has recently been reported by our laboratories which employs chemisorption by solid polyamine-based adsorbents. This method uses small amounts of silica-grafted polyethyleneimine to trap  $[^{11}\text{C}]\text{CO}_2$  at room temperature and quantitatively release it under mild heating (85 °C). Trapping efficiencies (TEs) as high as  $79 \pm 12\%$  were observed but decreased over multiple cycles, indicating a limited reusability of the capture material. This technology was applied to synthesize a PET tracer by  $[^{11}\text{C}]\text{CO}_2$  fixation reactions, and could potentially be applied for solid phase reactions as well as enable the transportation of carbon isotopes [23].

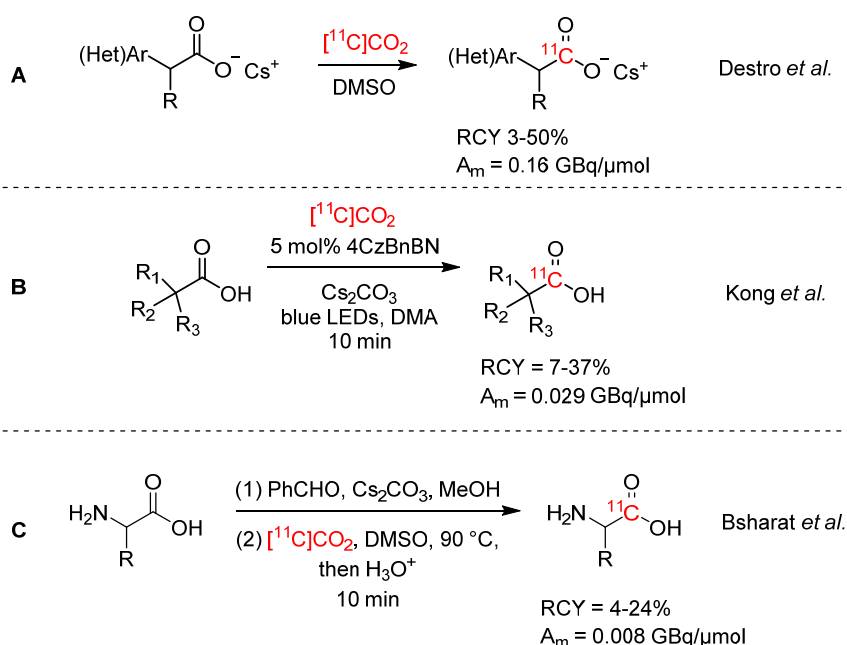
Traditionally, direct use of  $[^{11}\text{C}]\text{CO}_2$  is achieved by use of Grignard reagents, organolithiums or silanamines to yield  $^{11}\text{C}$ -labelled amides or carboxylic acids. However, these reagents are challenging to implement in automated PET tracer production due to their hygroscopic nature, tendency to absorb atmospheric  $\text{CO}_2$ , and corrosiveness [22]. As such, many new methodologies for the preparation of  $[^{11}\text{C}]$ carboxylic acids have been developed over the past five years by novel  $[^{11}\text{C}]\text{CO}_2$  fixation reactions that employ the aforementioned “fixation” bases. Our laboratory reported the use of aryl and heteroaryl stannanes as precursors which were carboxylated in a copper(I)-mediated reaction with  $[^{11}\text{C}]\text{CO}_2$  (see Scheme 2A) [24]. The method was fully automated and applied for an alternative synthesis of  $[^{11}\text{C}]$ bexarotene (previously synthesized by reaction of  $[^{11}\text{C}]\text{CO}_2$  with a boronic ester precursor mediated by a copper(I) source [25,26]), and was obtained with a RCY of  $32 \pm 5\%$  (decay-corrected (dc)) and a  $A_m$  of  $38 \pm 23$  GBq/ $\mu\text{mol}$ . The strategy was also applied by García-Vázquez et al. to the synthesis of  $^{11}\text{C}$ -carboxylated tetrazines for the labelling of trans-cyclooctene-functionalized PeptoBrushes [27]. After optimization of the original reaction conditions (CuI instead of CuTC, NMP instead of DMF and addition of TBAT as fluoride ion source), two tetrazines were successfully  $^{11}\text{C}$ -carboxylated with RCYs of 10–15% and “clicked” to the TCO-PeptoBrushes. It is noteworthy that Goudou et al. reported the copper-catalyzed radiosynthesis of  $[^{11}\text{C}]$ carboxylic acids by reaction of  $[^{11}\text{C}]\text{CO}_2$  with terminal alkynes in presence of DBU (see Scheme 2B) [28]. A small library of  $[^{11}\text{C}]$ propionic acids was obtained with RCYs between 7 and 28%. A different approach using trimethyl and trialkoxy silanes as precursor has been described by Bongarzone et al. (see Scheme 2C) [29]. In this desilylative carboxylation reaction, aromatic silane precursors were activated by fluoride, forming a pentavalent silicate which was then reacted in a copper-catalyzed reaction with  $[^{11}\text{C}]\text{CO}_2$ .  $[^{11}\text{C}]$ Carboxylic acids were obtained with RCYs of 19–93% and TEs of 21–89%. A more general approach for the synthesis of  $[^{11}\text{C}]$ carboxylic acids was introduced by Qu et al. (see Scheme 2D) [30].  $\text{sp}^-$ ,  $\text{sp}^2$ - and  $\text{sp}^3$ -hybridized carbon-attached trimethylsilanes were  $^{11}\text{C}$ -carboxylated in a fluoride-mediated desilylation (FMDS) reaction, resulting in a broad substrate scope and high RCYs (up to 98%). The applicability of the method was demonstrated by synthesizing two carboxylic acid PET tracers via the FMDS approach.

$[^{11}\text{C}]$ Carboxylic acids can also be synthesized by isotopic exchange reactions. Destro et al. reported the isotopic exchange reaction of cesium salt precursors with  $^{13}\text{C}$ ,  $^{14}\text{C}$ , and a few selected examples of  $^{11}\text{C}$  (see Scheme 3A) [31]. While good yields were obtained for  $[^{13}\text{C}]\text{CO}_2$  and  $[^{14}\text{C}]\text{CO}_2$ , yields were low for  $[^{11}\text{C}]\text{CO}_2$  (3–50%) due to low TEs. Another take on this strategy was demonstrated by Kong et al., who employed photoredox catalysis and obtained similar results (see Scheme 3B) [32]. In both cases,  $A_m$  was low, as expected ( $<0.2$  GBq/ $\mu\text{mol}$ ). A very recent addition to the portfolio of carboxylic acid labelling strategies by isotopic exchange was presented by Bsharat et al. [33]. These authors developed an aldehyde-catalyzed carboxylate exchange reaction in  $\alpha$ -amino acids (see Scheme 3C) with  $^{13}\text{C}$  and  $^{11}\text{C}$ . For the  $^{11}\text{C}$ -reactions, imine carboxylates were pre-formed by condensation of  $\alpha$ -amino acids with aryl aldehydes and subsequently subjected to the carboxylate exchange

reaction with  $[^{11}\text{C}]\text{CO}_2$ . An array of  $\alpha$ -amino acids was labelled with RCYs of 4–24%, and the modest yields were also attributed to low TEs of the  $[^{11}\text{C}]\text{CO}_2$ . Phenylalanine was isolated by this reaction with a  $A_m$  of 8.4 GBq/mmol.

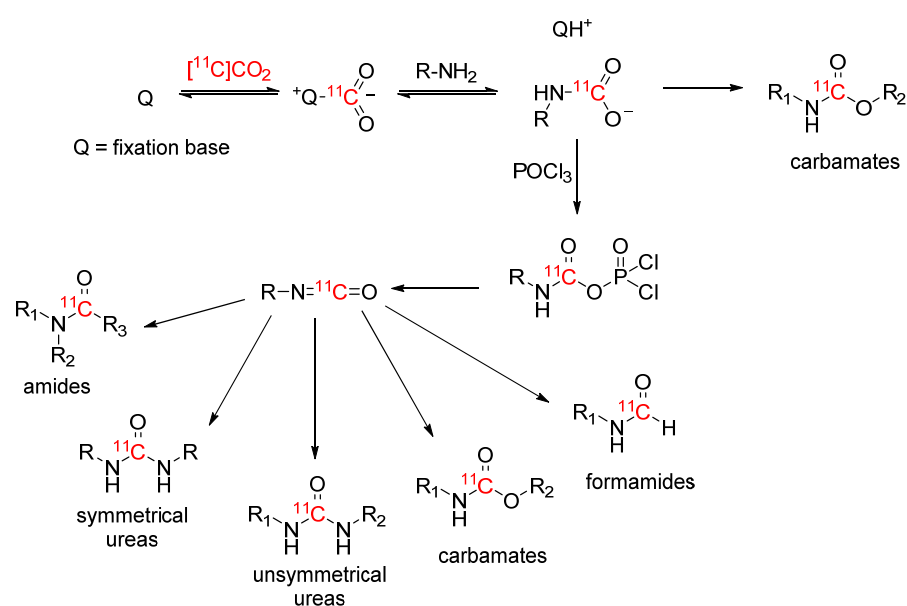


**Scheme 2.** New synthetic strategies for  $[^{11}\text{C}]\text{carboxylic acids}$  [24,28–30].



**Scheme 3.** Synthesis of  $[^{11}\text{C}]\text{carboxylic acids}$  via isotopic exchange [31–33].

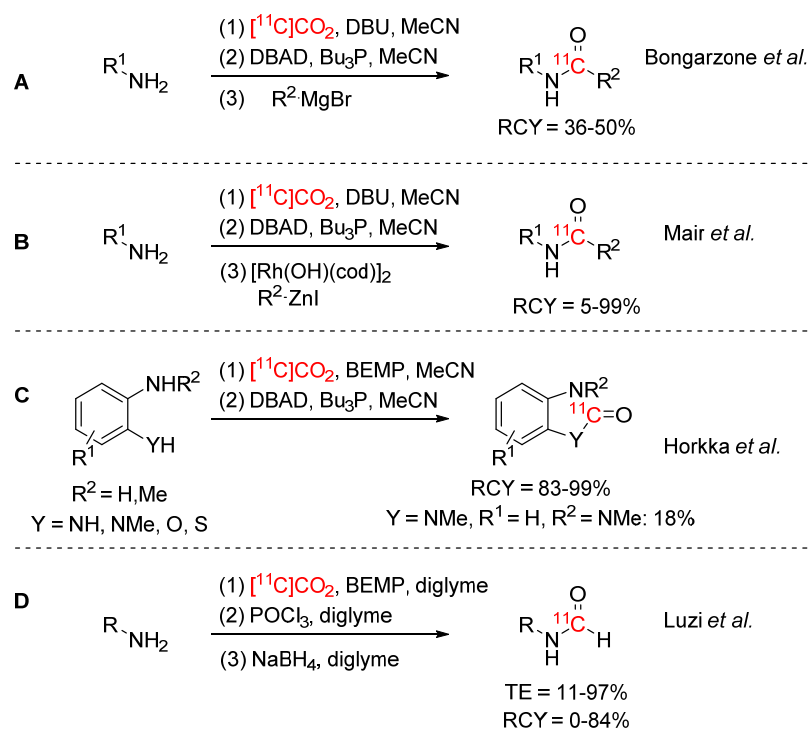
Scheme 4 gives an overview of the proposed mechanism of  $[^{11}\text{C}]\text{CO}_2$  fixation with fixation bases such as BEMP and DBU and formation of the  $[^{11}\text{C}]\text{isocyanate}$ , as well as the  $^{11}\text{C}$ -labelled functional groups that can be obtained via this pathway [18]. While early works focused on the synthesis of carbamates, the scope of  $^{11}\text{C}$ -labelled functional groups has broadened immensely over time.



**Scheme 4.** [ $^{11}\text{C}$ ]CO $_2$  fixation, [ $^{11}\text{C}$ ]isocyanate formation and  $^{11}\text{C}$ -products.

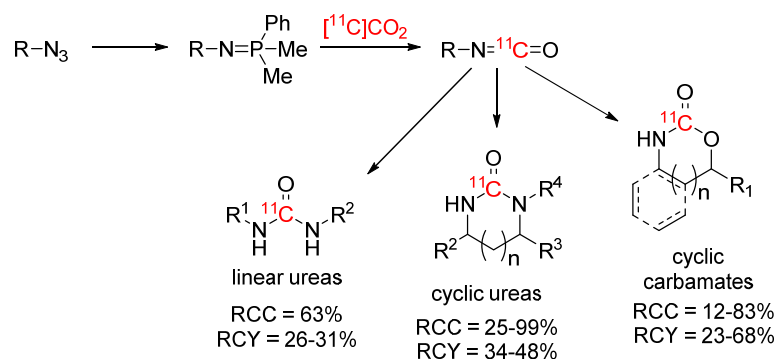
The efficient syntheses of carbon-11 labelled amides, ureas, and formamides have been a longstanding goal in PET radiochemistry and have seen an emergence of interest in recent years. Bongarzone et al. reported a rapid one-pot synthesis of amides via a Mitsunobu reaction (see Scheme 5A) [34]. [ $^{11}\text{C}$ ]CO $_2$  was trapped with DBU, converted to [ $^{11}\text{C}$ ]isocyanate (or an [ $^{11}\text{C}$ ]oxyphosphonium intermediate) using Mitsunobu reagents and subsequently reacted with a Grignard reagent to form the respective amide. RCYs of up to 50% were obtained. The substrate scope was not investigated for [ $^{11}\text{C}$ ]CO $_2$ , but [ $^{11}\text{C}$ ]melatonin was synthesized to demonstrate the applicability of this method to biologically relevant compounds. Mair et al. used organozinc iodides as alternatives to Grignard reagents in a rhodium-catalyzed addition to [ $^{11}\text{C}$ ]isocyanates (see Scheme 5B) [35]. The isocyanates were generated similarly to the previous method and reacted with the organozinc iodides in presence of a rhodium catalyst with RCYs of 5–99%. One model compound was isolated with a RCY of 12% and  $A_m$  of 267 GBq/ $\mu\text{mol}$  to demonstrate suitability for PET tracer production. In order to develop an efficient synthesis strategy for the benzimidazolone PET tracer (S)-[ $^{11}\text{C}$ ]CGP12177, Horkka et al. reported a BEMP/Mitsunobu-based strategy for the synthesis of cyclic aromatic ureas: *ortho*-Phenylenediamines were reacted with [ $^{11}\text{C}$ ]CO $_2$  in presence of BEMP as fixation base. Mitsunobu reagents (DBAD,  $n\text{Bu}_3\text{P}$ ) were added to form the [ $^{11}\text{C}$ ]isocyanate intermediates which then reacted intramolecularly to yield the respective  $^{11}\text{C}$ -labelled urea (see Scheme 5C) [36]. The strategy was also applied to cyclic carbamates and thiocarbamates, as well as the tracer (S)-[ $^{11}\text{C}$ ]CGP12177, which was obtained in 23% RCY (dc) with a  $A_m$  of 14 GBq/ $\mu\text{mol}$ . Luzi et al. reported the synthesis of [ $^{11}\text{C}$ ]formamides (see Scheme 5D) [37]. [ $^{11}\text{C}$ ]CO $_2$  was trapped with BEMP in diglyme and was reacted with aromatic and aliphatic primary amines to form the respective [ $^{11}\text{C}$ ]isocyanates, which were subsequently reduced to the [ $^{11}\text{C}$ ]formamides with sodium borohydride. The method performed better for aliphatic amines compared to aromatic amines.

In an attempt to make [ $^{11}\text{C}$ ]CO $_2$  fixation with BEMP and DBU more widely accessible and amenable to automation, two strategies of “in-loop” [ $^{11}\text{C}$ ]CO $_2$  fixation have been developed. While our laboratory developed this method using a standard stainless-steel HPLC loop for [ $^{11}\text{C}$ ]CO $_2$  fixation, Downey et al. applied a disposable ethylene tetrafluoroethylene loop [38,39]. In both cases, [ $^{11}\text{C}$ ]CO $_2$  was captured in the loop in the presence of an amine precursor and fixation base, prior to reaction with a model substrate. The “in-loop” fixation has been applied to synthesize  $^{11}\text{C}$ -labelled carbamates, unsymmetrical, and symmetrical ureas.



**Scheme 5.** Synthesis of [<sup>11</sup>C]amides and [<sup>11</sup>C]formamides via [<sup>11</sup>C]isocyanates [34–37].

A different approach to access ureas and carbamates via [<sup>11</sup>C]isocyanate was presented by Audisio and co-workers (see Scheme 6). The [<sup>11</sup>C]isocyanate intermediates were generated through a Staudinger aza-Wittig reaction from the respective azide, then reacted either intramolecularly to form cyclic [<sup>11</sup>C]ureas [40] and [<sup>11</sup>C]carbamates [41] or intermolecularly with an amine to form linear ureas [42]. All three strategies were applied for the synthesis of <sup>13</sup>C-, <sup>14</sup>C- and <sup>11</sup>C-labelled compounds. RCYs of the isolated <sup>11</sup>C-compounds generally ranged between 20 to 50%.

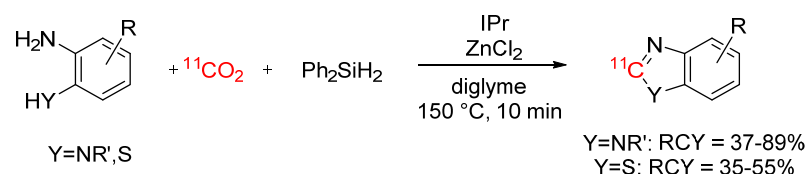


**Scheme 6.** <sup>11</sup>C-labelled ureas and carbamates via the Staudinger aza-Wittig reaction [40–42].

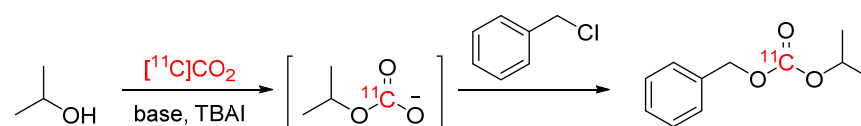
To avoid the multi-step syntheses and limited substrate scope of previously reported methods, Liger *et al.* reported a novel radiolabelling strategy for benzimidazoles and benzothiazoles (see Scheme 7). In this work, [<sup>11</sup>C]CO<sub>2</sub> was reacted with aromatic diamines and aminobenzenethiols in presence of 1,3-bis(2,6-diisopropylphenyl)imidazol-2-ylidene (IPr), zinc chloride, and phenylsilane as reducing reagent to obtain various benzimidazoles and benzothiazoles [43].

Previously, the synthesis of [<sup>11</sup>C]carbonates could only be achieved using the esoteric building block [<sup>11</sup>C]phosgene, which is technically challenging to prepare and requires specialized apparatus. To access this functional group directly from [<sup>11</sup>C]CO<sub>2</sub>, Dheere *et al.* developed a procedure involving an alkyl chloride, an alcohol, TBAI and base in DMF (see

Scheme 8) [44]. The procedure was used for the synthesis of one model compound, and resulted in either moderate RCY ( $31 \pm 2\%$ ) and higher  $A_m$  (10–20 GBq/ $\mu\text{mol}$ ; low amounts of  $^{11}\text{C}$ ), or high RCY (up to 82%) and lower  $A_m$  (2 GBq/ $\mu\text{mol}$ ), depending on the base.

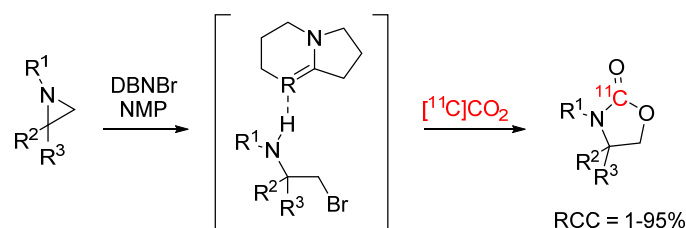


**Scheme 7.** Synthesis of carbon-11 labelled benzimidazoles and benzothiazoles [43].



**Scheme 8.** Synthesis of a  $^{11}\text{C}$  carbonate from  $^{11}\text{C}\text{CO}_2$  (RCY and  $A_m$  are base-dependent) [44].

A novel method for ring-opening non-activated aziridines with  $^{11}\text{C}\text{CO}_2$  using DBU/DBN halide ionic liquids was developed by our laboratory (see Scheme 9) [45].  $^{11}\text{C}\text{CO}_2$  was introduced to a pre-activated mixture of benzyl aziridine and the ionic liquid giving 4-benzyl  $^{11}\text{C}$ oxazolidinone-2-one with 77% radiochemical conversion (RCC) and 78% TE. The method was applied to radiolabel an array of  $^{11}\text{C}$ oxazolidinones (RCCs 5–95%) as well as a MAO-B inhibitor,  $^{11}\text{C}$ toloxatone, as a proof of concept.



**Scheme 9.** Ring-opening of non-activated aziridines with  $^{11}\text{C}\text{CO}_2$  [45].

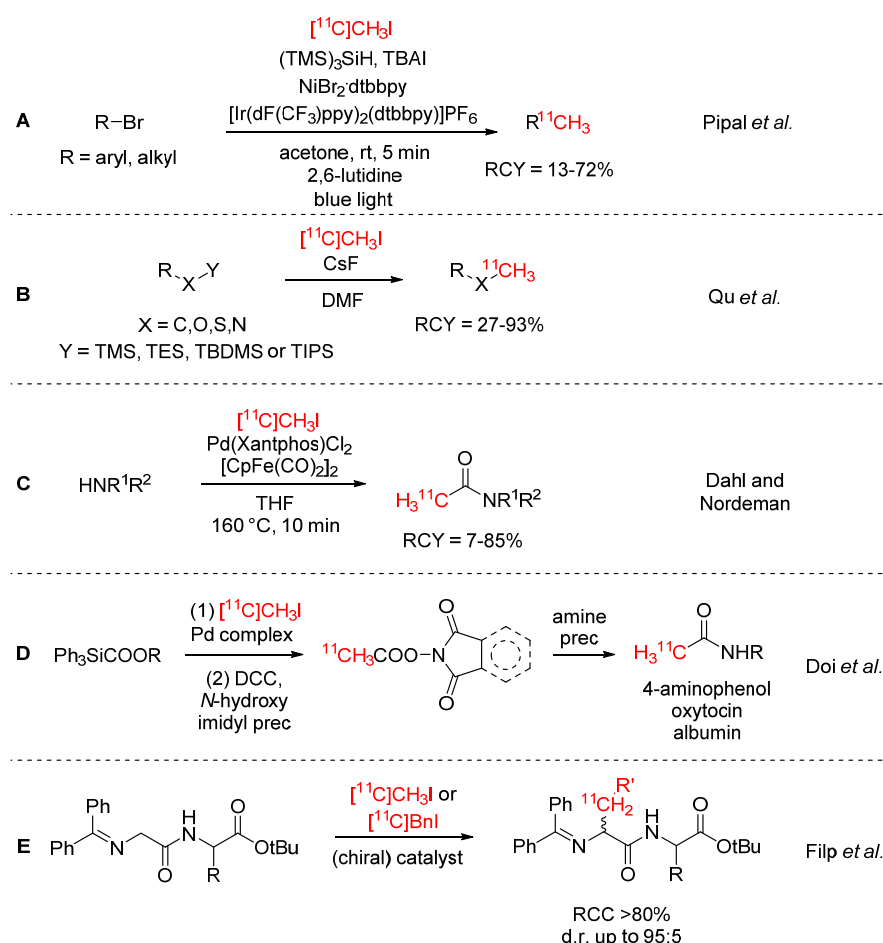
## 2.2. $^{11}\text{C}$ Carbon Monoxide

$^{11}\text{C}$ Carbon monoxide has gained much interest in recent years. Novel  $^{11}\text{C}\text{CO}$ -chemistry will not be covered within this review but we refer to recent comprehensive reviews of  $^{11}\text{C}\text{CO}$  production methods and  $^{11}\text{C}$ -carbonylation chemistry [46–50]. Although many straightforward routes for  $^{11}\text{C}\text{CO}$  production have been established, and a diverse portfolio of  $^{11}\text{C}$ carbonylation reactions has been developed, this branch of carbon-11 chemistry is still heavily underrepresented in PET tracer synthesis. In fact, of the 100+ labelled compounds synthesized from  $^{11}\text{C}\text{CO}$ , only four are reported for human use to our knowledge [51]. One likely reason for the hampered translation of  $^{11}\text{C}\text{CO}$  radiochemistry to the clinic can be attributed to the historic lack of commercially available automated synthesis units for  $^{11}\text{C}\text{CO}$ . This has now been overcome with systems such as the TracerMaker<sup>TM</sup> which is used by our laboratories for the syntheses of  $N$ - $^{11}\text{C}$ acrylamide PET tracers for imaging Bruton's tyrosine kinase via a palladium-NiXantphos-mediated carbonylation using  $^{11}\text{C}\text{CO}$  [51,52]. The synthesis of the same class of compounds has also recently been automated as “in-loop” procedure using the GE TracerLab synthesis modules [53]. Prior to this recent work,  $^{11}\text{C}$ -labelled  $N$ -acrylamides were synthesized from  $^{11}\text{C}$ acrylic acid or  $^{11}\text{C}$ acryloyl chloride (formed by carboxylation of Grignard or organolithium reagents with  $^{11}\text{C}\text{CO}_2$ ) and were not suitable for human translation.

## 2.3. $^{11}\text{C}$ Methyl Iodide and Other $^{11}\text{C}$ -Alkylation Agents

$^{11}\text{C}$ Methyl iodide and  $^{11}\text{C}$ methyl triflate have been known for many decades [54–57] and are by far the most commonly used  $^{11}\text{C}$ -labelling agents. Their widespread use is

attributed to their routine radiosyntheses and high reactivity. Both [ $^{11}\text{C}$ ]methyl iodide and [ $^{11}\text{C}$ ]methyl triflate can be easily synthesized from the primary cyclotron products (i.e., [ $^{11}\text{C}$ ]CH $_4$  or [ $^{11}\text{C}$ ]CO $_2$ ) using the classical wet-chemistry approach with lithium aluminium hydride and HI or the gas-phase method involving I $_2$ , and dedicated synthesis devices with fully automated procedures are commercially available [58]. Mostly, [ $^{11}\text{C}$ ]methyl iodide and [ $^{11}\text{C}$ ]methyl triflate are employed in  $^{11}\text{C}$ -methylation reactions of hydroxyl, amine or thiol precursors, but also many different  $^{11}\text{C}$ -C coupling reactions have been established, including Suzuki, Stille, and Negishi couplings. For an overview of  $^{11}\text{C}$ -C cross-coupling strategies, we refer the reader to a comprehensive review from H. Doi [59]. Recent progress in the field has been made by Rokka et al., who systematically studied the reaction of various organoborane precursors with [ $^{11}\text{C}$ ]methyl iodide in two different reaction media, DMF(/water) and THF/water, to determine the best precursor and solvent for Suzuki-type cross coupling reactions in  $^{11}\text{C}$ -chemistry [60]. These authors found that for their model compound (1-[ $^{11}\text{C}$ ]methylnaphthalene), the boronic acid and pinacol ester precursors gave the highest yields, while the solvent mixture THF/water was equal or superior in any tested reaction. Recent work focused on broadening the substrate scope to diversify  $^{11}\text{C}$ -methylation chemistry. Pipal et al. reported the  $^{11}\text{C}$ -methylation of aromatic and aliphatic bromides via metallaphotoredox catalysis (see Scheme 10A) [61]. The applicability of this labelling strategy was demonstrated by synthesizing 11  $^{11}\text{C}$ -labelled biologically active compounds, including the PET tracers [ $^{11}\text{C}$ ]UCB-J and [ $^{11}\text{C}$ ]PHNO, in RCYs of 13–72% for proof of concept. Qu et al. extended their fluoride-mediated desilylation of organosilanes, initially developed for [ $^{11}\text{C}$ ]CO $_2$  fixation (vide supra), to [ $^{11}\text{C}$ ]methyl iodide and succeeded in labelling a diverse library of silane substrates with RCYs of up to 93% (see Scheme 10B) [25].

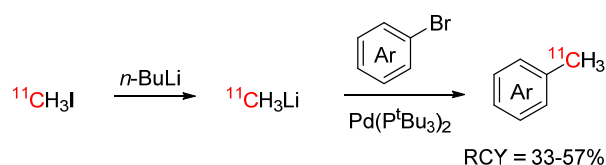


**Scheme 10.** Recent progress in [ $^{11}\text{C}$ ]CH $_3$ I chemistry [25,61–64].

As an alternative to [ $^{11}\text{C}$ ]CO or [ $^{11}\text{C}$ ]acetyl chloride chemistry, Dahl and Norde-man developed a procedure for  $^{11}\text{C}$ -acetylation of amines with [ $^{11}\text{C}$ ]methyl iodide (see Scheme 10C) [62]. Bis(cyclopentadienyldicarbonyliron) was used as the CO source in the Pd-mediated reaction. The reaction was established for a range of primary amine precursors, including three biologically relevant compounds, and a few examples of secondary amines. A different approach to the same functional group was presented by Doi et al., whereby [ $^{11}\text{C}$ ]acetic acid was synthesized in a palladium-mediated cross-coupling reaction from [ $^{11}\text{C}$ ]methyl iodide and carboxytriphenylsilane, then converted to the [ $^{11}\text{C}$ ]acetic acid phthalimidyl ester or succinimidyl ester (see Scheme 10D) [63]. The imidyl esters were subsequently employed in a  $^{11}\text{C}$ -acetylation reaction with small, medium-sized, and large molecules.

In an effort to develop a stereoselective  $^{11}\text{C}$ -alkylation procedure for diastereomerically enriched dipeptides, Filp et al. investigated the use of various quaternary ammonium salts as chiral phase-transfer catalysts in the  $^{11}\text{C}$ -alkylation of *N*-terminal glycine Schiff bases (see Scheme 10E) [64]. Next to [ $^{11}\text{C}$ ]methyl iodide, the procedure was also applied to [ $^{11}\text{C}$ ]benzyl iodide. RCCs of >80% and high diastereomeric ratios (d.r.) of up to 95:5 were obtained. A similar strategy has been used by Pekořak et al. for the stereoselective  $^{11}\text{C}$ -labelling of the tetrapeptide Phe-D-Trp-Lys-Thr with [ $^{11}\text{C}$ ]benzyl iodide [65]. [ $^{11}\text{C}$ ]Phe-D-Trp-Lys-Thr was synthesized over five steps starting from [ $^{11}\text{C}$ ]CO<sub>2</sub> and isolated with high stereoselectivity (94% de), RCYs of 9–10% (dc), and A<sub>m</sub> of 15–35 GBq/μmol.

To address the shortcomings of current cross-coupling strategies with [ $^{11}\text{C}$ ]methyl iodide, Helbert et al. developed a new cross-coupling procedure with [ $^{11}\text{C}$ ]methyl lithium. [ $^{11}\text{C}$ ]Methyl lithium was developed as a more reactive alternative for [ $^{11}\text{C}$ ]methyl iodide and can be synthesized by reaction of [ $^{11}\text{C}$ ]methyl iodide with *n*-butyllithium [66,67]. In the procedure of Herbert et al., [ $^{11}\text{C}$ ]methyl lithium was added without intermediate purification to the aryl bromide precursors and a selection of relevant PET tracers was labelled by palladium-mediated  $^{11}\text{C}$ -C cross-coupling with RCYs of 33–57% (see Scheme 11) [68].



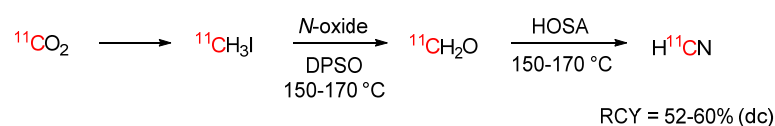
**Scheme 11.**  $^{11}\text{C}$ -C cross-coupling with [ $^{11}\text{C}$ ]methyl lithium [68].

#### 2.4. [ $^{11}\text{C}$ ]Hydrogen Cyanide

Since its inception in the 1960s [69], [ $^{11}\text{C}$ ]HCN has developed into a versatile building block for the  $^{11}\text{C}$ -labelling of neurotransmitters, amino acids, and other molecules. This is mainly due to its versatility: It can function as nucleophile as well as electrophile, and [ $^{11}\text{C}$ ]cyanide incorporation generates many different functionalities, such as nitriles, hydantoins, (thio)cyanates and, through subsequent reaction, carboxylic acids, aldehydes, amides and amines. Two extensive reviews on [ $^{11}\text{C}$ ]hydrogen cyanide have been recently published, therefore this  $^{11}\text{C}$ -building block will not be discussed in detail herein [70,71]. Since [ $^{11}\text{C}$ ]hydrogen cyanide is one of the few  $^{11}\text{C}$ -building blocks used for FIH PET tracers in recent years (vide infra), we will provide a brief summary of recent work that has not been covered by other reviews.

[ $^{11}\text{C}$ ]Hydrogen cyanide is typically produced by reacting [ $^{11}\text{C}$ ]CH<sub>4</sub> with NH<sub>3</sub> gas on a platinum catalyst at 1000 °C. While fully automated production systems are commercially available, [ $^{11}\text{C}$ ]HCN is not widely used. In an effort to make [ $^{11}\text{C}$ ]hydrogen cyanide more accessible, Kikuchi et al. developed a novel synthesis strategy from widely available [ $^{11}\text{C}$ ]methyl iodide (see Scheme 12) [72]. This method involves passing [ $^{11}\text{C}$ ]methyl iodide over a heated reaction column, in which it is first converted to [ $^{11}\text{C}$ ]formaldehyde and subsequently to [ $^{11}\text{C}$ ]hydrogen cyanide. The [ $^{11}\text{C}$ ]hydrogen cyanide is obtained fast and

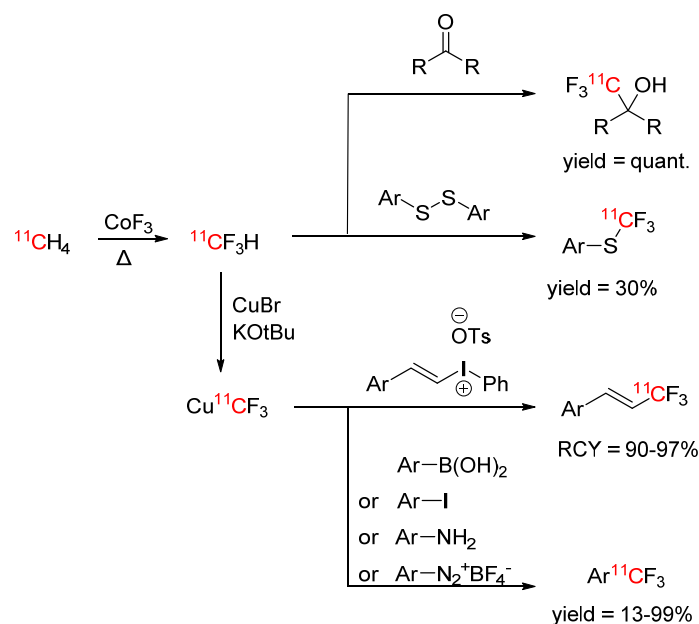
with RCYs comparable to the traditional method (50–60% at EOB), without the need for specialized equipment.



**Scheme 12.** Production of [ $^{11}\text{C}$ ]hydrogen cyanide from [ $^{11}\text{C}$ ]methyl iodide [72].

### 2.5. [ $^{11}\text{C}$ ]Fluoroform

Due to the prevalence of  $\text{CF}_3$  groups in drugs and other biologically active compounds, there has been much interest in labelling this group with carbon-11 and fluorine-18. Haskali et al. published a synthesis procedure for carbon-11 labelled fluoroform in 2017, where cyclotron-produced [ $^{11}\text{C}$ ]methane was fluorinated by passing it over a  $\text{CoF}_3$  column at elevated temperatures ( $270\text{ }^\circ\text{C}$ ) [73]. [ $^{11}\text{C}$ ]Fluoroform was obtained with RCYs of ~60%. The process was not only fast and reproducible, but the developed system also required very little maintenance. [ $^{11}\text{C}$ ]Fluoroform was reacted with various model compounds (see Scheme 13), in addition to three biologically active compounds.



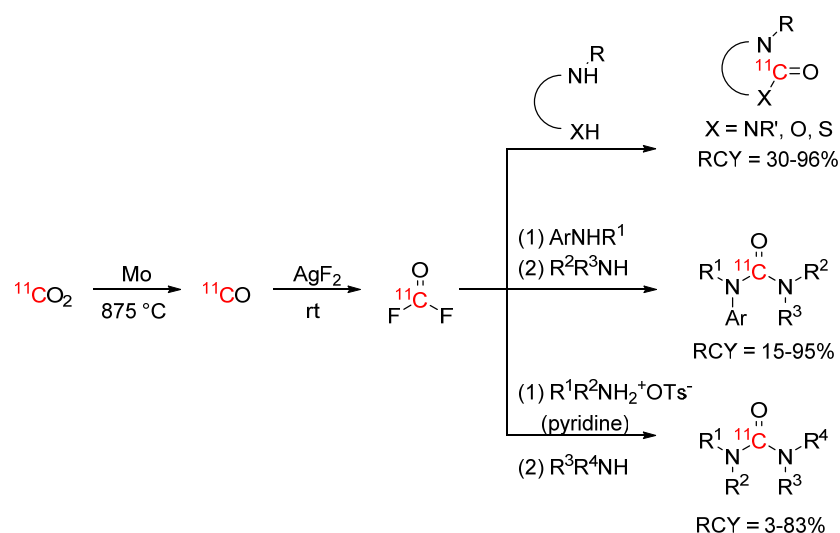
**Scheme 13.** [ $^{11}\text{C}$ ]Fluoroform chemistry [73–75].

Whereas fluorine-18 labelled fluoroform generally suffers from low molar activities ( $\leq 1\text{ GBq}/\mu\text{mol}$ ) and only few examples of higher molar activities are known, high molar activities of  $>200\text{ GBq}/\mu\text{mol}$  were easily obtained with carbon-11 labelled fluoroform. In later works, the substrate scope of reactions with [ $^{11}\text{C}$ ]fluoroform was broadened from aryl boronates, aryl iodides, ketones, diazonium salts, and diarylsulfanes to aryl amines and arylvinyl iodonium tosylates (see Scheme 13) [74,75].

### 2.6. [ $^{11}\text{C}$ ]Carbonyl Difluoride

As an alternative strategy to access carbon-11 labelled ureas, carbamates, and thiocarbamates, Jakobsson et al. presented the [ $^{11}\text{C}$ ]carbonyl group transfer agent [ $^{11}\text{C}$ ]carbonyl difluoride [76]. [ $^{11}\text{C}$ ]Carbonyl difluoride was synthesized quantitatively by passing [ $^{11}\text{C}$ ]CO over a  $\text{AgF}_2$  column at room temperature. The building block was subsequently reacted with diamines, aminoalcohols, and aminothiols to form the corresponding cyclic azolidin-2-ones (see Scheme 14) under mild conditions with very low precursor quantities, and even in presence of water. The same laboratory expanded their procedure to linear unsymmetrical

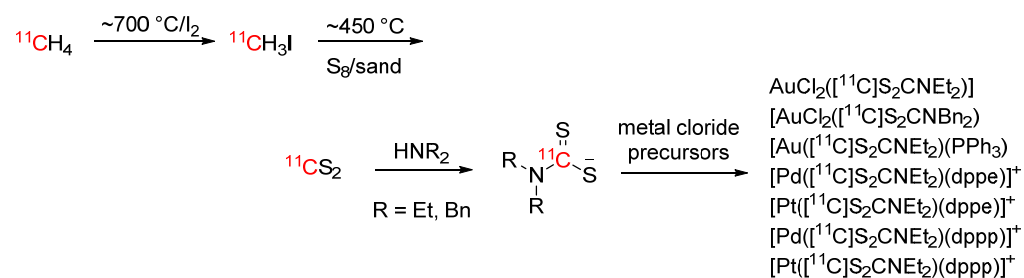
ureas and established reaction conditions for a broad scope of aryl and aliphatic amines [77]. For the aryl amines, [ $^{11}\text{C}$ ]carbonyl fluoride was trapped in a solution with the aryl amine precursor and subsequently reacted with another amine. For the aliphatic amines, alkylammonium tosylate precursors were used in the first step to lower the reactivity of the amine and prevent symmetrical urea formation. Pyridine was used to improve [ $^{11}\text{C}$ ]carbonyl fluoride trapping. Suitability for PET tracer synthesis was demonstrated by labelling the epoxide hydrolase inhibitor [ $^{11}\text{C}$ ]AR-9281, which was obtained after optimization in high RCYs of 80%.



**Scheme 14.** [ $^{11}\text{C}$ ]Carbonyl difluoride synthesis and subsequent reaction to cyclic products and linear unsymmetrical ureas [76,77].

### 2.7. [ $^{11}\text{C}$ ]Carbon Disulfide

[ $^{11}\text{C}$ ]Carbon disulfide, the sulfur analog of [ $^{11}\text{C}$ ]carbon dioxide, is an interesting  $^{11}\text{C}$ -building block for the synthesis of organosulfur compounds. It has first been described in 1984, and had limited utility until a decade ago when Miller and Bender proposed a new synthesis strategy, which was further improved by Haywood et al. [78–80]. It can now be readily obtained through the reaction of [ $^{11}\text{C}$ ]CH $_3$ I with elemental sulfur and has been used to synthesize [ $^{11}\text{C}$ ]thioureas, thiocarbamates and related structures. Cesarc et al. recently published a procedure for the synthesis of late transition metal complexes with [ $^{11}\text{C}$ ]dithiocarbamate ligands [81]. To this end, [ $^{11}\text{C}$ ]carbon disulfide was reacted with diethyl amine or dibenzyl amine to form the respective ammonium [ $^{11}\text{C}$ ]dithiocarbamate salt and subsequently reacted with Au(I), Au(III), Pd(II) or Pt(II) complexes to form the respective complexes in RCYs > 70% (see Scheme 15).

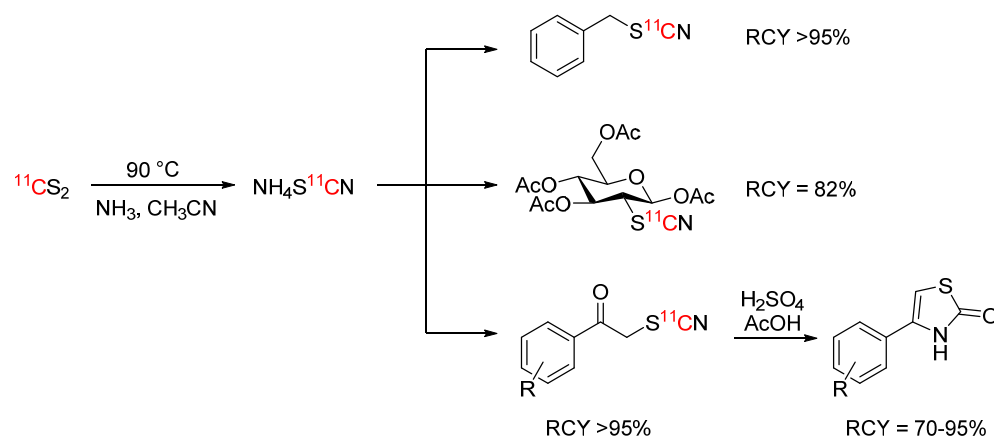


**Scheme 15.** Synthesis of [ $^{11}\text{C}$ ]carbon disulfide and formation of [ $^{11}\text{C}$ ]dithiocarbamate transition metal complexes [81].

### 2.8. [ $^{11}\text{C}$ ]Thiocyanate

[ $^{11}\text{C}$ ]Thiocyanate is an interesting  $^{11}\text{C}$ -building block because of its reactivity and potential to give access to a wide range of organosulfur derivatives. Up until recently,

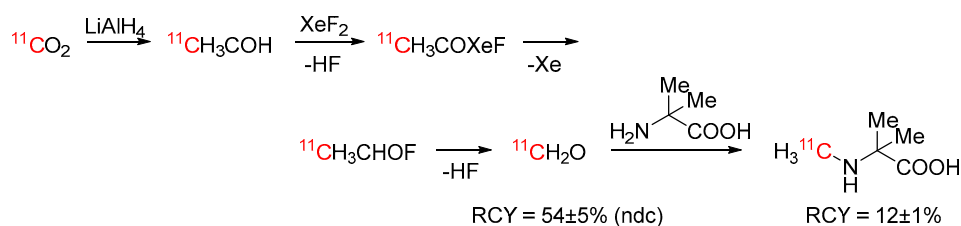
its production relied on the use of  $[^{11}\text{C}]\text{HCN}$  [82]. Haywood et al. presented a new way to synthesize this  $^{11}\text{C}$ -building block by reacting  $[^{11}\text{C}]\text{carbon disulfide}$  with ammonia at  $90\text{ }^\circ\text{C}$  to form ammonium  $[^{11}\text{C}]\text{thiocyanate}$  in near quantitative RCC [83]. The ammonium  $[^{11}\text{C}]\text{thiocyanate}$  was subsequently reacted with benzyl bromide, a range of  $\alpha$ -ketobromides, and mannose triflate in high RCYs of  $\geq 75\%$  (see Scheme 16). The  $\alpha$ - $[^{11}\text{C}]\text{thiocyanatophenones}$  could also be cyclized in the presence of sulfuric and acetic acid to  $^{11}\text{C}$ -thiazolones.



**Scheme 16.** Synthesis of and reactions with ammonium  $[^{11}\text{C}]\text{thiocyanate}$  [83].

### 2.9. $[^{11}\text{C}]\text{Formaldehyde}$

$[^{11}\text{C}]\text{Formaldehyde}$  is an established and versatile building block for carbon-11 chemistry (see [84] and references therein). Many different synthetic strategies have been proposed, traditionally involving reduction in cyclotron-produced  $[^{11}\text{C}]\text{CO}_2$  to  $[^{11}\text{C}]\text{CH}_3\text{OH}$  and subsequent oxidation to  $[^{11}\text{C}]\text{formaldehyde}$ . Nader et al. recently proposed the use of  $\text{XeF}_2$  as an oxidizing agent (see Scheme 17) [85].  $[^{11}\text{C}]\text{Formaldehyde}$  was obtained in non-decay corrected RCYs of  $54 \pm 5\%$  starting from  $[^{11}\text{C}]\text{CO}_2$  and was used in a proof-of-principle synthesis to form  $\alpha$ -( $N$ - $[^{11}\text{C}]\text{methylamino}$ )isobutyric acid via reductive  $^{11}\text{C}$ -methylation.



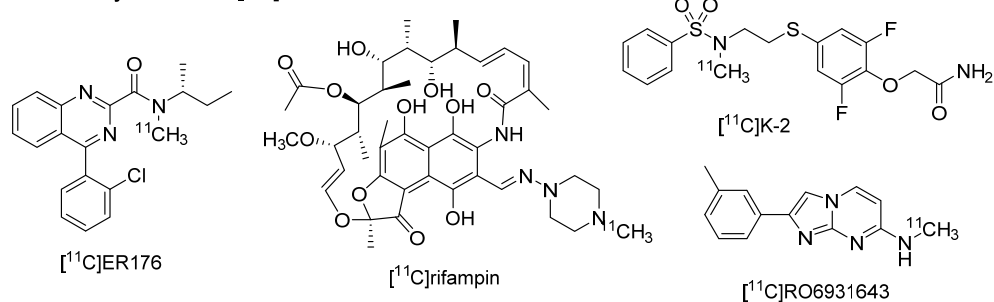
**Scheme 17.** Synthesis of  $[^{11}\text{C}]\text{formaldehyde}$  using  $\text{XeF}_2$  as oxidizing agent and reaction to  $[^{11}\text{C}]\text{Me-AIB}$  [85].

### 3. First-in-Human Translation

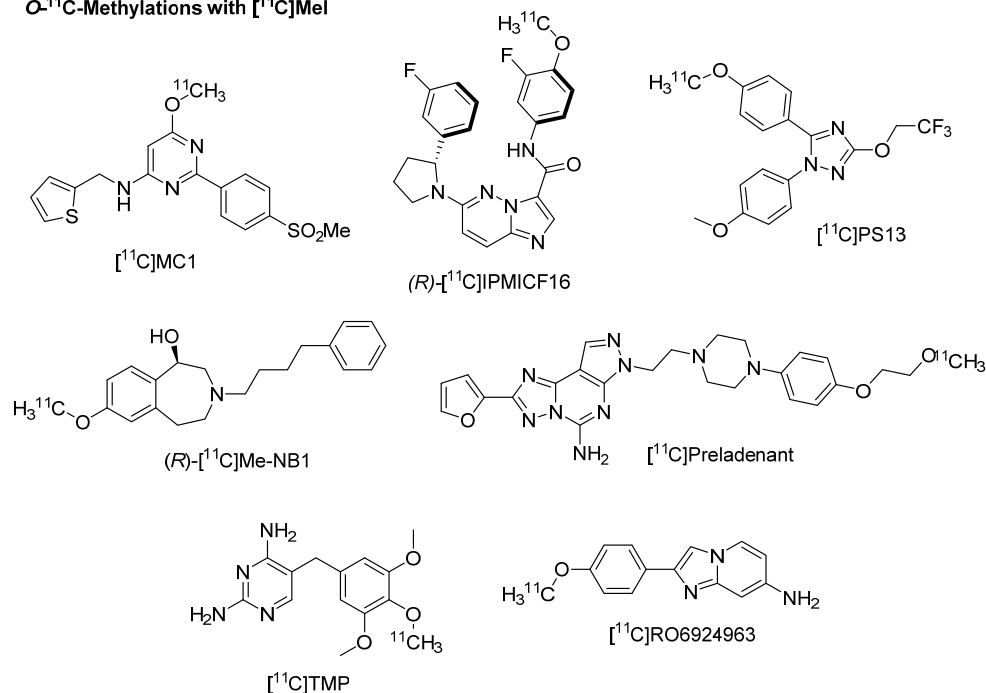
Despite the short physical half-life and the need for an on-site cyclotron,  $^{11}\text{C}$  continues to be a favoured radionuclide for small molecule PET tracers. As discussed in this review, innovations continue in  $^{11}\text{C}$ -radiolabelling strategies for applications in  $^{11}\text{C}$ -tracer development. Within the past five years, to our knowledge at least 27 novel  $^{11}\text{C}$ -labelled PET tracers have been translated for FIH PET studies (see Figure 1) [86–109]. Unsurprisingly, the vast majority of these PET tracers were designed to image targets within the CNS (see Table 1). Carbon-11 is ideal for CNS PET because the substitution of naturally occurring  $^{12}\text{C}$  with  $^{11}\text{C}$  does not change the physicochemical properties of the compound, thereby enabling imaging with isotopologues of the molecules of interest for accurate determination of brain penetrance, target affinity, pharmacokinetics, or pharmacodynamics of the molecule, and multiple scans can be performed in the same subject in the same day. Interestingly, many

of the  $^{11}\text{C}$ -labelled PET tracers for FIH use focused on imaging markers of neuroinflammation, a critical component in the etiology and pathology of several neurodegenerative diseases, including Alzheimer's disease (AD), Parkinson's disease (PD), and amyotrophic lateral sclerosis (ALS) [110–114]. The remaining PET tracers translated for FIH studies that were reported in the past five years strived to image non-CNS targets, including bacterial infection and lung inflammation.

#### N- $^{11}\text{C}$ -Methylations with [ $^{11}\text{C}$ ]MeI



#### O- $^{11}\text{C}$ -Methylations with [ $^{11}\text{C}$ ]MeI



#### Other $^{11}\text{C}$ -methylations with [ $^{11}\text{C}$ ]MeI

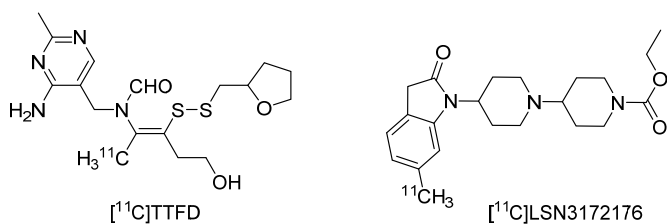
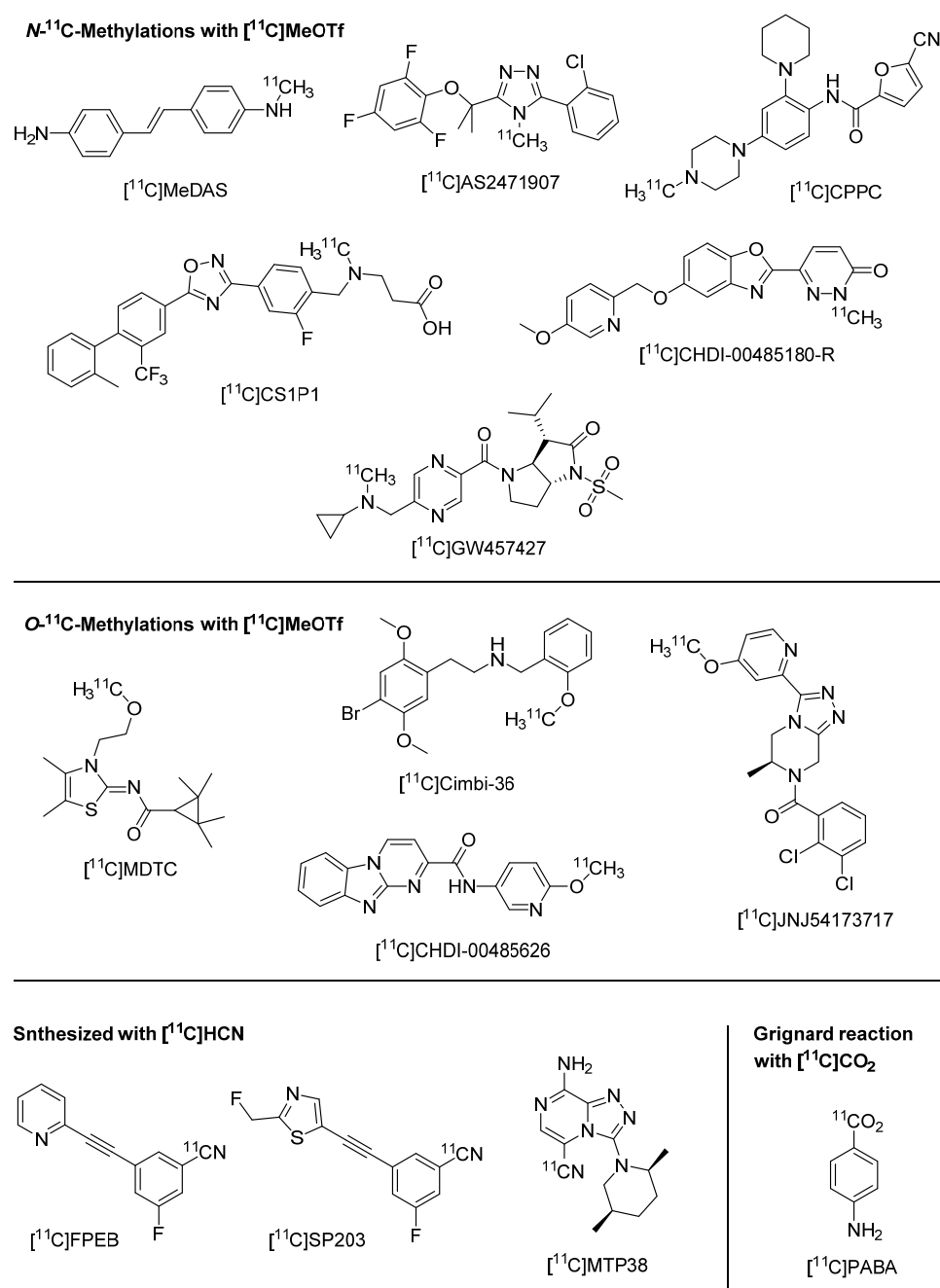


Figure 1. Cont.



**Figure 1.** Chemical structures of the majority of first-in-human PET tracers labelled with <sup>11</sup>C since 2017. Targets, publication years and references of the tracers are listed in Table 1.

When sorting the tracers according to the labelling method, it becomes immediately apparent that the predominant synthetic strategy remains <sup>11</sup>C-methylation of hydroxy or amino precursors: more than  $\frac{3}{4}$  of all tracers were synthesized via this strategy, either using [<sup>11</sup>C]methyl iodide or [<sup>11</sup>C]methyl triflate as the <sup>11</sup>C-building block (see Figure 2). This can be attributed to the accessibility of these building blocks from cyclotron-produced [<sup>11</sup>C]CO<sub>2</sub> or [<sup>11</sup>C]CH<sub>4</sub> and the availability of commercial synthesis devices (vide supra) [58]. Other tracers have been synthesized by alternate <sup>11</sup>C-labelling strategies, using [<sup>11</sup>C]HCN or Grignard reactions with [<sup>11</sup>C]CO<sub>2</sub>. The latest developments in <sup>11</sup>C-chemistry are not represented among the FIH tracers, which is not surprising since it usually takes time for a new method to be implemented by the broader community. However, many of the existing <sup>11</sup>C-building blocks have not been introduced in the past few years but have been around for decades and should, therefore, be available for clinical application. As indicated in some

cases (e.g., [ $^{11}\text{C}$ ]CO chemistry), it may be the historic lack of specialized or commercially available radiosynthesis equipment that hampers FIH translation of new PET tracers. Other reasons could be that new  $^{11}\text{C}$ -methodologies are often only developed up to the point of proof-of-principle and not optimized for automated tracer production. Rather than further broadening the scope of  $^{11}\text{C}$ -chemistry, future efforts should focus on closing the gap between new method development and clinical translation.

**Table 1.** First-in-human  $^{11}\text{C}$  PET tracers and their targets reported since 2017.

Tracer	Target	$^{11}\text{C}$ -Building Block	Year	Ref.
[ $^{11}\text{C}$ ]ER176	TSPO	[ $^{11}\text{C}$ ]CH <sub>3</sub> I	2017	[92]
[ $^{11}\text{C}$ ]K-2	AMPA receptors	[ $^{11}\text{C}$ ]CH <sub>3</sub> I	2020	[96]
[ $^{11}\text{C}$ ]rifampin	Tuberculosis meningitis	[ $^{11}\text{C}$ ]CH <sub>3</sub> I	2018	[105]
[ $^{11}\text{C}$ ]MC1	COX-2	[ $^{11}\text{C}$ ]CH <sub>3</sub> I	2020	[98]
(R)-[ $^{11}\text{C}$ ]IPMICF16	TrkB/C receptors	[ $^{11}\text{C}$ ]CH <sub>3</sub> I	2017	[87]
[ $^{11}\text{C}$ ]RO6924963	Tau	[ $^{11}\text{C}$ ]CH <sub>3</sub> I	2018	[109]
[ $^{11}\text{C}$ ]RO6931643	Tau	[ $^{11}\text{C}$ ]CH <sub>3</sub> I	2018	[109]
(R)-[ $^{11}\text{C}$ ]Me-NB1	GluN2B-containing NMDA receptors	[ $^{11}\text{C}$ ]CH <sub>3</sub> I	2022	[86]
[ $^{11}\text{C}$ ]Preladenant	Adenosine A <sub>2A</sub> receptors	[ $^{11}\text{C}$ ]CH <sub>3</sub> I	2017	[103]
[ $^{11}\text{C}$ ]TMP	Bacterial infection	[ $^{11}\text{C}$ ]CH <sub>3</sub> I	2021	[107]
[ $^{11}\text{C}$ ]PS13	COX-1	[ $^{11}\text{C}$ ]CH <sub>3</sub> I	2020	[104]
[ $^{11}\text{C}$ ]TTFD	Drug pharmacokinetics	[ $^{11}\text{C}$ ]CH <sub>3</sub> I	2021	[108]
[ $^{11}\text{C}$ ]LSN3172176	M1 muscarinic acetylcholine receptors	[ $^{11}\text{C}$ ]CH <sub>3</sub> I	2020	[97]
[ $^{11}\text{C}$ ]MeDAS	Myelin	[ $^{11}\text{C}$ ]MeOTf	2022	[100]
[ $^{11}\text{C}$ ]AS2471907	11 $\beta$ -hydroxysteroid dehydrogenase type 1	[ $^{11}\text{C}$ ]MeOTf	2019	[88]
[ $^{11}\text{C}$ ]CPPC	CSF1 receptor	[ $^{11}\text{C}$ ]MeOTf	2022	[91]
[ $^{11}\text{C}$ ]CS1P1	Sphingosine-1-phosphate receptor 1	[ $^{11}\text{C}$ ]MeOTf	2022	[93]
[ $^{11}\text{C}$ ]CHDI-00485180-R	mHTT	[ $^{11}\text{C}$ ]MeOTf	2022	[89]
[ $^{11}\text{C}$ ]GW457427	Neutrophil elastase	[ $^{11}\text{C}$ ]MeOTf	2022	[94]
[ $^{11}\text{C}$ ]MDTC	CB2 receptor	[ $^{11}\text{C}$ ]MeOTf	2022	[99]
[ $^{11}\text{C}$ ]Cimbi-36	5-HT <sub>2A</sub> receptor	[ $^{11}\text{C}$ ]MeOTf	2019	[90]
[ $^{11}\text{C}$ ]CHDI-00485626	mHTT	[ $^{11}\text{C}$ ]MeOTf	2022	[89]
[ $^{11}\text{C}$ ]JNJ54173717	P2X7 receptor	[ $^{11}\text{C}$ ]MeOTf	2019	[95]
[ $^{11}\text{C}$ ]FPEB	mGluR5	[ $^{11}\text{C}$ ]HCN	2017	[106]
[ $^{11}\text{C}$ ]SP203	mGluR5	[ $^{11}\text{C}$ ]HCN	2017	[106]
[ $^{11}\text{C}$ ]MTP38	PDE7	[ $^{11}\text{C}$ ]HCN	2021	[101]
[ $^{11}\text{C}$ ]PABA	Renal imaging	[ $^{11}\text{C}$ ]CO <sub>2</sub>	2020	[102]

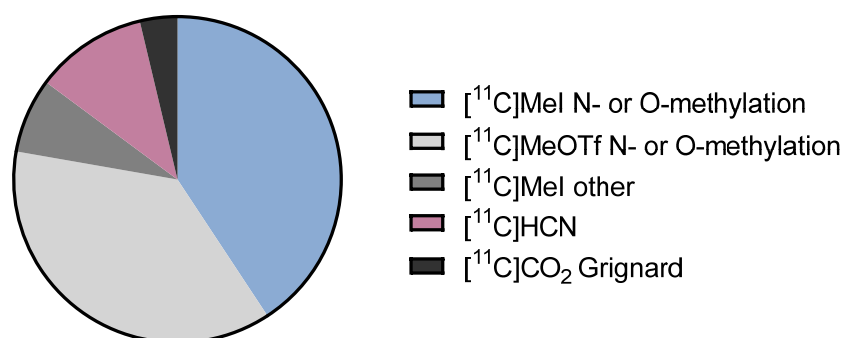


**Figure 2.** Graphical representation of the proportions of  $^{11}\text{C}$ -labelling strategies used for FIH PET tracers since 2017.

**Author Contributions:** Conceptualization, A.P. and N.V.; writing—original draft preparation, A.P.; writing—review and editing, M.C., A.L. and N.V.; visualization, A.P.; supervision, N.V. All authors have read and agreed to the published version of the manuscript.

**Funding:** A.P. is supported by the CAMH Discovery Fund. M.C. was supported by the Canadian Institute for Health Research with a Canadian Graduate Scholarship (CGS-M), as well as a Mitacs Accelerate Internship award provided by the Structural Genomics Consortium (SGC). N.V. is supported by the Azrieli Foundation, the Canada Research Chairs Program, Canada Foundation for Innovation and the Ontario Research Fund.

**Institutional Review Board Statement:** Not applicable.

**Informed Consent Statement:** Not applicable.

**Data Availability Statement:** Not applicable.

**Conflicts of Interest:** The authors declare no relevant conflict of interest.

## Abbreviations

4CzBnBN	(2,3,4,6)-3-Benzyl-2,4,5,6-tetra(9H-carbazol-9-yl)benzotrile
5-HT <sub>2A</sub> receptor	5-Hydroxy-tryptamine 2A receptor
AD	Alzheimer's disease
ALS	Amyotrophic lateral sclerosis
A <sub>m</sub>	Molar activity
AMPA receptor	α-amino-3-hydroxy-5-methyl-4-isoxazolepropionic acid receptor
BEMP	2- <i>tert</i> -butylimino-2-diethylamino-1,3-dimethylperhydro-1,3,2-diazaphosphorine
CB2 receptor	Cannabinoid receptor type 2
CNS	Central nervous system
COX-1, -2	Cyclooxygenase-1, -2
CSF1	colony stimulating factor 1
CuTC	Copper(I) thiophene-2-carboxylate
DBAD	Di- <i>tert</i> -butyl azodicarboxylate
DBN	1,5-Diazabicyclo [4.3.0]non-5-ene
DBU	1,8-diazabicyclo [5.4.0]undec-7-ene
dc	Decay-corrected
DCC	<i>N,N'</i> -Dicyclohexylcarbodiimide
de	Diastereomeric excess
DMA	Dimethylacetamide
DMF	Dimethylformamide
DMSO	Dimethyl sulfoxide
DPSO	Diphenyl sulfoxide
d.r.	Diastereomeric ratio
dtbbpy	4,4'-Di- <i>tert</i> -butyl-2,2'-bipyridine
FIH	First-in-human
FMDS	Fluoride-mediated desilylation
HOSA	Hydroxylamine- <i>O</i> -sulfonic acid
HPLC	High-performance liquid chromatography
IPr	1,3-bis(2,6-diisopropylphenyl)imidazol-2-ylidene)
K <sub>222</sub>	4,7,13,16,21,24-Hexaoxa-1,10-diazabicyclo [8.8.8]hexacosane
MAO-B	Monoamine oxidase B
mGluR5	Metabotropic glutamate receptor 5
mHTT	Mutant huntingtin protein
NMDA	<i>N</i> -methyl-D-aspartate
NMP	<i>N</i> -Methyl-2-pyrrolidone
PD	Parkinson's disease
PDE7	Phosphodiesterase 7
PET	Positron emission tomography
ppy	2-Phenylpyridine
prec	precursor

quant.	quantitative
RCC	Radiochemical conversion
RCP	Radiochemical purity
RCY	Radiochemical yield
Ref.	Reference
rt	Room temperature
$t_{1/2}$	Half-life
TBAT	Tetrabutylammonium difluorotriphenylsilicate
TBAI	Tetra- <i>n</i> -butylammonium iodide
TE	Trapping efficiency
THF	Tetrahydrofuran
TMEDA	Tetramethylethylenediamine
TMS	Trimethylsilyl
TrkB/C	Tropomyosin receptor kinase B/C
TSPO	Translocator protein

## References

- Liang, S.H.; Vasdev, N. Total Radiosynthesis: Thinking Outside ‘the Box’. *Aust. J. Chem.* **2015**, *68*, 1319–1328. [[CrossRef](#)] [[PubMed](#)]
- Deng, X.; Rong, J.; Wang, L.; Vasdev, N.; Zhang, L.; Josephson, L.; Liang, S.H. Chemistry for Positron Emission Tomography: Recent Advances in  $^{11}\text{C}$ -,  $^{18}\text{F}$ -,  $^{13}\text{N}$ -, and  $^{15}\text{O}$ -Labeling Reactions. *Angew. Chem. Int. Ed.* **2019**, *58*, 2580–2605. [[CrossRef](#)]
- Ajenjo, J.; Destro, G.; Cornelissen, B.; Gouverneur, V. Closing the Gap between  $^{19}\text{F}$  and  $^{18}\text{F}$  Chemistry. *EJNMMI Radiopharm. Chem.* **2021**, *6*, 33. [[CrossRef](#)]
- Van der Born, D.; Pees, A.; Poot, A.J.; Orru, R.V.A.; Windhorst, A.D.; Vugts, D.J. Fluorine-18 Labelled Building Blocks for PET Tracer Synthesis. *Chem. Soc. Rev.* **2017**, *46*, 4709–4773. [[CrossRef](#)] [[PubMed](#)]
- Bernard-Gauthier, V.; Lepage, M.L.; Waengler, B.; Bailey, J.J.; Liang, S.H.; Perrin, D.M.; Vasdev, N.; Schirrmacher, R. Recent Advances in  $^{18}\text{F}$  Radiochemistry: A Focus on B- $^{18}\text{F}$ , Si- $^{18}\text{F}$ , Al- $^{18}\text{F}$ , and C- $^{18}\text{F}$  Radiofluorination via Spirocyclic Iodonium Ylides. *J. Nucl. Med.* **2018**, *59*, 568–572. [[CrossRef](#)]
- Goud, N.S.; Joshi, R.K.; Bharath, R.D.; Kumar, P. Fluorine-18: A Radionuclide with Diverse Range of Radiochemistry and Synthesis Strategies for Target Based PET Diagnosis. *Eur. J. Med. Chem.* **2020**, *187*, 111979. [[CrossRef](#)] [[PubMed](#)]
- Wang, Y.; Lin, Q.; Shi, H.; Cheng, D. Fluorine-18: Radiochemistry and Target-Specific PET Molecular Probes Design. *Front. Chem.* **2022**, *10*, 884517. [[CrossRef](#)]
- Bratteby, K.; Shalgunov, V.; Herth, M.M. Aliphatic  $^{18}\text{F}$ -Radiofluorination: Recent Advances in the Labeling of Base-Sensitive Substrates. *ChemMedChem* **2021**, *16*, 2612–2622. [[CrossRef](#)]
- Francis, F.; Wuest, F. Advances in [ $^{18}\text{F}$ ]Trifluoromethylation Chemistry for PET Imaging. *Molecules* **2021**, *26*, 6478. [[CrossRef](#)]
- Wright, J.S.; Kaur, T.; Preshlock, S.; Tanzey, S.S.; Winton, W.P.; Sharninghausen, L.S.; Wiesner, N.; Brooks, A.F.; Sanford, M.S.; Scott, P.J.H. Copper-Mediated Late-Stage Radiofluorination: Five Years of Impact on Preclinical and Clinical PET Imaging. *Clin. Transl. Imaging* **2020**, *8*, 167–206. [[CrossRef](#)]
- Bui, T.T.; Kim, H. Recent Advances in Photo-mediated Radiofluorination. *Chem. Asian J.* **2021**, *16*, 2155–2167. [[CrossRef](#)]
- Goud, N.S.; Bhattacharya, A.; Joshi, R.K.; Nagaraj, C.; Bharath, R.D.; Kumar, P. Carbon-11: Radiochemistry and Target-Based PET Molecular Imaging Applications in Oncology, Cardiology, and Neurology. *J. Med. Chem.* **2021**, *64*, 1223–1259. [[CrossRef](#)] [[PubMed](#)]
- Boscutti, G.; Huiban, M.; Passchier, J. Use of Carbon-11 Labelled Tool Compounds in Support of Drug Development. *Drug Discov. Today Technol.* **2017**, *25*, 3–10. [[CrossRef](#)] [[PubMed](#)]
- Dahl, K.; Halldin, C.; Schou, M. New Methodologies for the Preparation of Carbon-11 Labeled Radiopharmaceuticals. *Clin. Transl. Imaging* **2017**, *5*, 275–289. [[CrossRef](#)] [[PubMed](#)]
- Rotstein, B.H.; Liang, S.H.; Placzek, M.S.; Hooker, J.M.; Gee, A.D.; Dollé, F.; Wilson, A.A.; Vasdev, N.  $^{11}\text{C}=\text{O}$  Bonds Made Easily for Positron Emission Tomography Radiopharmaceuticals. *Chem. Soc. Rev.* **2016**, *45*, 4708–4726. [[CrossRef](#)]
- Pike, V.W. PET Radiotracers: Crossing the Blood–Brain Barrier and Surviving Metabolism. *Trends Pharmacol. Sci.* **2009**, *30*, 431–440. [[CrossRef](#)]
- Coenen, H.H.; Gee, A.D.; Adam, M.; Antoni, G.; Cutler, C.S.; Fujibayashi, Y.; Jeong, J.M.; Mach, R.H.; Mindt, T.L.; Pike, V.W.; et al. Consensus Nomenclature Rules for Radiopharmaceutical Chemistry—Setting the Record Straight. *Nucl. Med. Biol.* **2017**, *55*, v–xi. [[CrossRef](#)]
- Herth, M.M.; Ametamey, S.; Antuganov, D.; Bauman, A.; Berndt, M.; Brooks, A.F.; Bormans, G.; Choe, Y.S.; Gillings, N.; Häfeli, U.O.; et al. On the Consensus Nomenclature Rules for Radiopharmaceutical Chemistry—Reconsideration of Radiochemical Conversion. *Nucl. Med. Biol.* **2021**, *93*, 19–21. [[CrossRef](#)]
- Hooker, J.M.; Reibel, A.T.; Hill, S.M.; Schueller, M.J.; Fowler, J.S. One-Pot, Direct Incorporation of [ $^{11}\text{C}$ ]CO<sub>2</sub> into Carbamates. *Angew. Chem. Int. Ed.* **2009**, *48*, 3482–3485. [[CrossRef](#)]
- Wilson, A.A.; Garcia, A.; Houle, S.; Sadvovskii, O.; Vasdev, N. Synthesis and Application of Isocyanates Radiolabeled with Carbon-11. *Chem. Eur. J.* **2011**, *17*, 259–264. [[CrossRef](#)]

21. Wilson, A.A.; Garcia, A.; Houle, S.; Vasdev, N. Direct Fixation of [ $^{11}\text{C}$ ]CO $_2$  by Amines: Formation of [ $^{11}\text{C}$ -Carbonyl]-Methylcarbamates. *Org. Biomol. Chem.* **2010**, *8*, 428–432. [[CrossRef](#)] [[PubMed](#)]
22. Rotstein, B.H.; Liang, S.H.; Holland, J.P.; Collier, T.L.; Hooker, J.M.; Wilson, A.A.; Vasdev, N.  $^{11}\text{C}$ CO $_2$  Fixation: A Renaissance in PET Radiochemistry. *Chem. Commun.* **2013**, *49*, 5621–5629. [[CrossRef](#)]
23. Chassé, M.; Sen, R.; Goeppert, A.; Prakash, G.K.S.; Vasdev, N. Polyamine Based Solid CO $_2$  Adsorbents for [ $^{11}\text{C}$ ]CO $_2$  Purification and Radiosynthesis. *J. CO $_2$  Util.* **2022**, *64*, 102137. [[CrossRef](#)]
24. Duffy, I.R.; Vasdev, N.; Dahl, K. Copper(I)-Mediated  $^{11}\text{C}$ -Carboxylation of (Hetero)Arylstannanes. *ACS Omega* **2020**, *5*, 8242–8250. [[CrossRef](#)]
25. Riss, P.J.; Lu, S.; Telu, S.; Aigbirhio, F.I.; Pike, V.W. CuI-Catalyzed  $^{11}\text{C}$  Carboxylation of Boronic Acid Esters: A Rapid and Convenient Entry to  $^{11}\text{C}$ -Labeled Carboxylic Acids, Esters, and Amides. *Angew. Chem. Int. Ed.* **2012**, *51*, 2698–2702. [[CrossRef](#)]
26. Rotstein, B.H.; Hooker, J.M.; Woo, J.; Collier, T.L.; Brady, T.J.; Liang, S.H.; Vasdev, N. Synthesis of [ $^{11}\text{C}$ ]Bexarotene by Cu-Mediated [ $^{11}\text{C}$ ]Carbon Dioxide Fixation and Preliminary PET Imaging. *ACS Med. Chem. Lett.* **2014**, *5*, 668–672. [[CrossRef](#)]
27. García-Vázquez, R.; Battisti, U.M.; Shalgunov, V.; Schäfer, G.; Barz, M.; Herth, M.M. [ $^{11}\text{C}$ ]Carboxylated Tetrazines for Facile Labeling of Trans-Cyclooctene-Functionalized PeptoBrushes. *Macromol. Rapid Commun.* **2022**, *43*, 2100655. [[CrossRef](#)]
28. Goudou, F.; Gee, A.D.; Bongarzone, S. Carbon-11 Carboxylation of Terminal Alkynes with [ $^{11}\text{C}$ ]CO $_2$ . *J. Label. Compd. Radiopharm.* **2021**, *64*, 237–242. [[CrossRef](#)]
29. Bongarzone, S.; Raucchi, N.; Fontana, I.C.; Luzi, F.; Gee, A.D. Carbon-11 Carboxylation of Trialkoxysilane and Trimethylsilane Derivatives Using [ $^{11}\text{C}$ ]CO $_2$ . *Chem. Commun.* **2020**, *56*, 4668–4671. [[CrossRef](#)]
30. Qu, W.; Hu, B.; Babich, J.W.; Waterhouse, N.; Dooley, M.; Ponnala, S.; Urgiles, J. A General  $^{11}\text{C}$ -Labeling Approach Enabled by Fluoride-Mediated Desilylation of Organosilanes. *Nat. Commun.* **2020**, *11*, 1736. [[CrossRef](#)]
31. Destro, G.; Horkka, K.; Loreau, O.; Buisson, D.; Kingston, L.; Del Vecchio, A.; Schou, M.; Elmore, C.S.; Taran, F.; Cantat, T.; et al. Transition-Metal-Free Carbon Isotope Exchange of Phenyl Acetic Acids. *Angew. Chem.* **2020**, *132*, 13592–13597. [[CrossRef](#)]
32. Kong, D.; Munch, M.; Qiqige, Q.; Cooze, C.J.C.; Rotstein, B.H.; Lundgren, R.J. Fast Carbon Isotope Exchange of Carboxylic Acids Enabled by Organic Photoredox Catalysis. *J. Am. Chem. Soc.* **2021**, *143*, 2200–2206. [[CrossRef](#)] [[PubMed](#)]
33. Bsharat, O.; Doyle, M.G.J.; Munch, M.; Mair, B.A.; Cooze, C.J.C.; Derdau, V.; Bauer, A.; Kong, D.; Rotstein, B.H.; Lundgren, R.J. Aldehyde-Catalysed Carboxylate Exchange in  $\alpha$ -Amino Acids with Isotopically Labelled CO $_2$ . *Nat. Chem.* **2022**, *14*, 1367–1374. [[CrossRef](#)]
34. Bongarzone, S.; Runser, A.; Taddei, C.; Dheere, A.K.H.; Gee, A.D. From [ $^{11}\text{C}$ ]CO $_2$  to [ $^{11}\text{C}$ ]Amides: A Rapid One-Pot Synthesis via the Mitsunobu Reaction. *Chem. Commun.* **2017**, *53*, 5334–5337. [[CrossRef](#)]
35. Mair, B.A.; Fouad, M.H.; Ismailani, U.S.; Munch, M.; Rotstein, B.H. Rhodium-Catalyzed Addition of Organozinc Iodides to Carbon-11 Isocyanates. *Org. Lett.* **2020**, *22*, 2746–2750. [[CrossRef](#)]
36. Horkka, K.; Dahl, K.; Bergare, J.; Elmore, C.S.; Halldin, C.; Schou, M. Rapid and Efficient Synthesis of  $^{11}\text{C}$ -Labeled Benzimidazolones Using [ $^{11}\text{C}$ ]Carbon Dioxide. *ChemistrySelect* **2019**, *4*, 1846–1849. [[CrossRef](#)]
37. Luzi, F.; Gee, A.D.; Bongarzone, S. Rapid One-Pot Radiosynthesis of [Carbonyl- $^{11}\text{C}$ ]Formamides from Primary Amines and [ $^{11}\text{C}$ ]CO $_2$ . *EJNMMI Radiopharm. Chem.* **2020**, *5*, 20. [[CrossRef](#)]
38. Dahl, K.; Collier, T.L.; Cheng, R.; Zhang, X.; Sadvovski, O.; Liang, S.H.; Vasdev, N. “In-Loop” [ $^{11}\text{C}$ ]CO $_2$  Fixation: Prototype and Proof of Concept. *J. Label. Compd. Radiopharm.* **2018**, *61*, 252–262. [[CrossRef](#)]
39. Downey, J.; Bongarzone, S.; Hader, S.; Gee, A.D. In-Loop Flow [ $^{11}\text{C}$ ]CO $_2$  Fixation and Radiosynthesis of *N,N'*-[ $^{11}\text{C}$ ]Dibenzylurea. *J. Label. Compd. Radiopharm.* **2018**, *61*, 263–271. [[CrossRef](#)]
40. Del Vecchio, A.; Caillé, F.; Chevalier, A.; Loreau, O.; Horkka, K.; Halldin, C.; Schou, M.; Camus, N.; Kessler, P.; Kuhnast, B.; et al. Late-Stage Isotopic Carbon Labeling of Pharmaceutically Relevant Cyclic Ureas Directly from CO $_2$ . *Angew. Chem.* **2018**, *130*, 9892–9896. [[CrossRef](#)]
41. Del Vecchio, A.; Talbot, A.; Caillé, F.; Chevalier, A.; Sallustrau, A.; Loreau, O.; Destro, G.; Taran, F.; Audisio, D. Carbon Isotope Labeling of Carbamates by Late-Stage [ $^{11}\text{C}$ ], [ $^{13}\text{C}$ ] and [ $^{14}\text{C}$ ]Carbon Dioxide Incorporation. *Chem. Commun.* **2020**, *56*, 11677–11680. [[CrossRef](#)]
42. Babin, V.; Sallustrau, A.; Loreau, O.; Caillé, F.; Goudet, A.; Cahuzac, H.; Del Vecchio, A.; Taran, F.; Audisio, D. A General Procedure for Carbon Isotope Labeling of Linear Urea Derivatives with Carbon Dioxide. *Chem. Commun.* **2021**, *57*, 6680–6683. [[CrossRef](#)] [[PubMed](#)]
43. Liger, F.; Cadarossanesaib, F.; Jecker, T.; Tourvieille, C.; Le Bars, D.; Billard, T.  $^{11}\text{C}$ -Labeling: Intracyclic Incorporation of Carbon-11 into Heterocycles:  $^{11}\text{C}$ -Labeling: Intracyclic Incorporation of Carbon-11 into Heterocycles. *Eur. J. Org. Chem.* **2019**, *2019*, 6968–6972. [[CrossRef](#)]
44. Haji Dheere, A.K.; Bongarzone, S.; Shakir, D.; Gee, A. Direct Incorporation of [ $^{11}\text{C}$ ]CO $_2$  into Asymmetric [ $^{11}\text{C}$ ]Carbonates. *J. Chem.* **2018**, *2018*, 7641304. [[CrossRef](#)]
45. Lindberg, A.; Vasdev, N. Ring-Opening of Non-Activated Aziridines with [ $^{11}\text{C}$ ]CO $_2$  via Novel Ionic Liquids. *RSC Adv.* **2022**, *12*, 21417–21421. [[CrossRef](#)] [[PubMed](#)]
46. Taddei, C.; Pike, V.W. [ $^{11}\text{C}$ ]Carbon Monoxide: Advances in Production and Application to PET Radiotracer Development over the Past 15 Years. *EJNMMI Radiopharm. Chem.* **2019**, *4*, 25. [[CrossRef](#)] [[PubMed](#)]
47. Eriksson, J.; Antoni, G.; Långström, B.; Itsenko, O. The Development of  $^{11}\text{C}$ -Carboxylation Chemistry: A Systematic View. *Nucl. Med. Biol.* **2021**, *92*, 115–137. [[CrossRef](#)]

48. Nielsen, D.U.; Neumann, K.T.; Lindhardt, A.T.; Skrydstrup, T. Recent Developments in Carbonylation Chemistry Using [ $^{13}\text{C}$ ]CO, [ $^{11}\text{C}$ ]CO, and [ $^{14}\text{C}$ ]CO. *J. Label. Compd. Radiopharm.* **2018**, *61*, 949–987. [[CrossRef](#)]
49. Taddei, C.; Gee, A.D. Recent Progress in [ $^{11}\text{C}$ ]Carbon Dioxide ([ $^{11}\text{C}$ ]CO<sub>2</sub>) and [ $^{11}\text{C}$ ]Carbon Monoxide ([ $^{11}\text{C}$ ]CO) Chemistry. *J. Label. Compd. Radiopharm.* **2018**, *61*, 237–251. [[CrossRef](#)]
50. Shegani, A.; Kealey, S.; Luzi, F.; Basagni, F.; Machado, J.D.M.; Ekici, S.D.; Ferocino, A.; Gee, A.D.; Bongarzone, S. Radiosynthesis, Preclinical, and Clinical Positron Emission Tomography Studies of Carbon-11 Labeled Endogenous and Natural Exogenous Compounds. *Chem. Rev.* **2023**, *123*, 105–229. [[CrossRef](#)] [[PubMed](#)]
51. Dahl, K.; Turner, T.; Vasdev, N. Radiosynthesis of a Bruton's Tyrosine Kinase Inhibitor, [ $^{11}\text{C}$ ]Tolbrutinib, via Palladium-NiXantphos-mediated Carbonylation. *J. Label. Compd. Radiopharm.* **2020**, *63*, 482–487. [[CrossRef](#)] [[PubMed](#)]
52. Lindberg, A.; Boyle, A.J.; Tong, J.; Harkness, M.B.; Garcia, A.; Tran, T.; Zhai, D.; Liu, F.; Donnelly, D.J.; Vasdev, N. Radiosynthesis of [ $^{11}\text{C}$ ]Ibrutinib via Pd-Mediated [ $^{11}\text{C}$ ]CO Carbonylation: Preliminary PET Imaging in Experimental Autoimmune Encephalomyelitis Mice. *Front. Nucl. Med.* **2021**, *1*, 772289. [[CrossRef](#)]
53. Donnelly, D.J.; Preshlock, S.; Kaur, T.; Tran, T.; Wilson, T.C.; Mhanna, K.; Henderson, B.D.; Batalla, D.; Scott, P.J.H.; Shao, X. Synthesis of Radiopharmaceuticals via "In-Loop"  $^{11}\text{C}$ -Carbonylation as Exemplified by the Radiolabeling of Inhibitors of Bruton's Tyrosine Kinase. *Front. Nucl. Med.* **2022**, *1*, 820235. [[CrossRef](#)]
54. Langstrom, B.; Lundqvist, H. The Preparation of  $^{11}\text{C}$ -Methyl Iodide and Its Use in the Synthesis of  $^{11}\text{C}$ -Methyl-Methionine. *Int. J. Appl. Radiat. Isot.* **1976**, *27*, 357–363. [[CrossRef](#)] [[PubMed](#)]
55. Comar, D.; Cartron, J.-C.; Maziere, M.; Marazano, C. Labelling and Metabolism of Methionine-Methyl- $^{11}\text{C}$ . *Eur. J. Nucl. Med.* **1976**, *1*, 11–14. [[CrossRef](#)]
56. Marazano, C.; Maziere, M.; Berger, G.; Comar, D. Synthesis of Methyl Iodide- $^{11}\text{C}$  and Formaldehyde- $^{11}\text{C}$ . *Int. J. Appl. Radiat. Isot.* **1977**, *28*, 49–52. [[CrossRef](#)]
57. Jewett, D.M. A Simple Synthesis of [ $^{11}\text{C}$ ]Methyl Triflate. *Appl. Radiat. Isot.* **1992**, *43*, 1383–1385. [[CrossRef](#)]
58. Mock, B. Automated C-11 Methyl Iodide/Triflate Production: Current State of the Art. *Curr. Org. Chem.* **2013**, *17*, 2119–2126. [[CrossRef](#)]
59. Doi, H. Pd-Mediated Rapid Cross-Couplings Using [ $^{11}\text{C}$ ]Methyl Iodide: Groundbreaking Labeling Methods in  $^{11}\text{C}$  Radiochemistry: Development of Pd-Mediated Rapid C-[ $^{11}\text{C}$ ]Methylations. *J. Label. Compd. Radiopharm.* **2015**, *58*, 73–85. [[CrossRef](#)]
60. Rokka, J.; Nordeman, P.; Roslin, S.; Eriksson, J. A Comparative Study on Suzuki-type  $^{11}\text{C}$ -methylation of Aromatic Organoboranes Performed in Two Reaction Media. *J. Label. Compd. Radiopharm.* **2021**, *64*, 447–455. [[CrossRef](#)]
61. Pipal, R.W.; Stout, K.T.; Musacchio, P.Z.; Ren, S.; Graham, T.J.A.; Verhoog, S.; Gantert, L.; Lohith, T.G.; Schmitz, A.; Lee, H.S.; et al. Metallaphotoredox Aryl and Alkyl Radiomethylation for PET Ligand Discovery. *Nature* **2021**, *589*, 542–547. [[CrossRef](#)]
62. Dahl, K.; Nordeman, P.  $^{11}\text{C}$ -Acetylation of Amines with [ $^{11}\text{C}$ ]Methyl Iodide with Bis(Cyclopentadienyldicarbonyliron) as the CO Source:  $^{11}\text{C}$ -Acetylation of Amines with [ $^{11}\text{C}$ ]Methyl Iodide with Bis(Cyclopentadienyldicarbonyliron) as the CO Source. *Eur. J. Org. Chem.* **2017**, *2017*, 5785–5788. [[CrossRef](#)]
63. Doi, H.; Goto, M.; Sato, Y. Pd<sup>0</sup>-Mediated Cross-Coupling of [ $^{11}\text{C}$ ]Methyl Iodide with Carboxysilane for Synthesis of [ $^{11}\text{C}$ ]Acetic Acid and Its Active Esters:  $^{11}\text{C}$ -Acetylation of Small, Medium, and Large Molecules. *Eur. J. Org. Chem.* **2021**, *2021*, 3970–3979. [[CrossRef](#)]
64. Filip, U.; Pekošak, A.; Poot, A.J.; Windhorst, A.D. Stereocontrolled [ $^{11}\text{C}$ ]Alkylation of N-Terminal Glycine Schiff Bases To Obtain Dipeptides: Stereocontrolled [ $^{11}\text{C}$ ]Alkylation of N-Terminal Glycine Schiff Bases To Obtain Dipeptides. *Eur. J. Org. Chem.* **2017**, *2017*, 5592–5596. [[CrossRef](#)]
65. Pekošak, A.; Rotstein, B.H.; Collier, T.L.; Windhorst, A.D.; Vasdev, N.; Poot, A.J. Stereoselective  $^{11}\text{C}$  Labeling of a "Native" Tetrapeptide by Using Asymmetric Phase-Transfer Catalyzed Alkylation Reactions. *Eur. J. Org. Chem.* **2017**, *2017*, 1019–1024. [[CrossRef](#)]
66. Reiffers, S.; Vaalburg, W.; Wiegman, T.; Wynberg, H.; Woldring, M.G. Carbon-11 Labelled Methylolithium as Methyl Donating Agent: The Addition to 17-Keto Steroids. *Int. J. Appl. Radiat. Isot.* **1980**, *31*, 535–539. [[CrossRef](#)]
67. Berger, G.; Maziere, M.; Prenant, C.; Sastre, J.; Comar, D. Synthesis of High Specific Activity  $^{11}\text{C}$  17alpha Methyltestosterone. *Int. J. Appl. Radiat. Isot.* **1981**, *32*, 811–815. [[CrossRef](#)]
68. Helbert, H.; Antunes, I.F.; Luurtsema, G.; Szymanski, W.; Feringa, B.L.; Elsinga, P.H. Cross-Coupling of [ $^{11}\text{C}$ ]Methylolithium for  $^{11}\text{C}$ -Labelled PET Tracer Synthesis. *Chem. Commun.* **2021**, *57*, 203–206. [[CrossRef](#)]
69. Dubrin, J.; MacKay, C.; Pandow, M.L.; Wolfgang, R. Reactions of Atomic Carbon with Pi-Bonded Inorganic Molecules. *J. Inorg. Nucl. Chem.* **1964**, *26*, 2113–2122. [[CrossRef](#)]
70. Xu, Y.; Qu, W. [ $^{11}\text{C}$ ]HCN Radiochemistry: Recent Progress and Future Perspectives. *Eur. J. Org. Chem.* **2021**, *2021*, 4653–4682. [[CrossRef](#)]
71. Zhou, Y.-P.; Makaravage, K.J.; Brugarolas, P. Radiolabeling with [ $^{11}\text{C}$ ]HCN for Positron Emission Tomography. *Nucl. Med. Biol.* **2021**, *102–103*, 56–86. [[CrossRef](#)] [[PubMed](#)]
72. Kikuchi, T.; Ogawa, M.; Okamura, T.; Gee, A.D.; Zhang, M.-R. Rapid 'on-Column' Preparation of Hydrogen [ $^{11}\text{C}$ ]Cyanide from [ $^{11}\text{C}$ ]Methyl Iodide via [ $^{11}\text{C}$ ]Formaldehyde. *Chem. Sci.* **2022**, *13*, 3556–3562. [[CrossRef](#)] [[PubMed](#)]
73. Haskali, M.B.; Pike, V.W. [ $^{11}\text{C}$ ]Fluoroform, a Breakthrough for Versatile Labeling of PET Radiotracer Trifluoromethyl Groups in High Molar Activity. *Chem. Eur. J.* **2017**, *23*, 8156–8160. [[CrossRef](#)] [[PubMed](#)]

74. Jana, S.; Telu, S.; Yang, B.Y.; Haskali, M.B.; Jakobsson, J.E.; Pike, V.W. Rapid Syntheses of [<sup>11</sup>C]Arylvinyltrifluoromethanes through Treatment of (*E*)-Arylvinyl(Phenyl)Iodonium Tosylates with [<sup>11</sup>C]Trifluoromethylcopper(I). *Org. Lett.* **2020**, *22*, 4574–4578. [[CrossRef](#)] [[PubMed](#)]
75. Young, N.J.; Pike, V.W.; Taddei, C. Rapid and Efficient Synthesis of [<sup>11</sup>C]Trifluoromethylarenes from Primary Aromatic Amines and [<sup>11</sup>C]CuCF<sub>3</sub>. *ACS Omega* **2020**, *5*, 19557–19564. [[CrossRef](#)]
76. Jakobsson, J.E.; Lu, S.; Telu, S.; Pike, V.W. [<sup>11</sup>C]Carbonyl Difluoride—A New and Highly Efficient [<sup>11</sup>C]Carbonyl Group Transfer Agent. *Angew. Chem. Int. Ed.* **2020**, *59*, 7256–7260. [[CrossRef](#)]
77. Jakobsson, J.E.; Telu, S.; Lu, S.; Jana, S.; Pike, V.W. Broad Scope and High-Yield Access to Unsymmetrical Acyclic [<sup>11</sup>C]Ureas for Biomedical Imaging from [<sup>11</sup>C]Carbonyl Difluoride. *Chem. Eur. J.* **2021**, *27*, 10369–10376. [[CrossRef](#)]
78. Niisawa, K.; Ogawa, K.; Saito, J.; Taki, K.; Karasawa, T.; Nozaki, T. Production of No-Carrier-Added <sup>11</sup>C-Carbon Disulfide and <sup>11</sup>C-Hydrogen Cyanide by Microwave Discharge. *Int. J. Appl. Radiat. Isot.* **1984**, *35*, 29–33. [[CrossRef](#)]
79. Miller, P.W.; Bender, D. [<sup>11</sup>C]Carbon Disulfide: A Versatile Reagent for PET Radiolabelling. *Chem. Eur. J.* **2012**, *18*, 433–436. [[CrossRef](#)]
80. Haywood, T.; Kealey, S.; Sánchez-Cabezas, S.; Hall, J.J.; Allott, L.; Smith, G.; Plisson, C.; Miller, P.W. Carbon-11 Radiolabelling of Organosulfur Compounds: <sup>11</sup>C Synthesis of the Progesterone Receptor Agonist Tanaproget. *Chem. Eur. J.* **2015**, *21*, 9034–9038. [[CrossRef](#)]
81. Cesarec, S.; Edgar, F.; Lai, T.; Plisson, C.; White, A.J.P.; Miller, P.W. Synthesis of Carbon-11 Radiolabelled Transition Metal Complexes Using <sup>11</sup>C-Dithiocarbamates. *Dalton Trans.* **2022**, *51*, 5004–5008. [[CrossRef](#)]
82. Stone-Elander, S.; Roland, P.; Halldin, C.; Hassan, M.; Seitz, R. Synthesis of [<sup>11</sup>C]Sodium Thiocyanate for In Vivo Studies of Anion Kinetics Using Positron Emission Tomography (PET). *Nucl. Med. Biol.* **1989**, *16*, 741–746. [[CrossRef](#)]
83. Haywood, T.; Cesarec, S.; Kealey, S.; Plisson, C.; Miller, P.W. Ammonium [<sup>11</sup>C]Thiocyanate: Revised Preparation and Reactivity Studies of a Versatile Nucleophile for Carbon-11 Radiolabelling. *Med. Chem. Commun.* **2018**, *9*, 1311–1314. [[CrossRef](#)] [[PubMed](#)]
84. Hooker, J.M.; Schönberger, M.; Schieferstein, H.; Fowler, J.S. A Simple, Rapid Method for the Preparation of [<sup>11</sup>C]Formaldehyde. *Angew. Chem. Int. Ed.* **2008**, *47*, 5989–5992. [[CrossRef](#)] [[PubMed](#)]
85. Nader, M.; Oberdorfer, F.; Herrmann, K. Production of [<sup>11</sup>C]Formaldehyde by the XeF<sub>2</sub> Mediated Oxidation of [<sup>11</sup>C]Methanol and Its Application in the Labeling of α-(N-[<sup>11</sup>C]Methylamino)isobutyric Acid. *Appl. Radiat. Isot.* **2019**, *148*, 178–183. [[CrossRef](#)] [[PubMed](#)]
86. Rischka, L.; Vraka, C.; Pichler, V.; Rasul, S.; Nics, L.; Gryglewski, G.; Handschuh, P.; Murgaš, M.; Godbersen, G.M.; Silberbauer, L.R.; et al. First-in-Humans Brain PET Imaging of the GluN2B-Containing N-Methyl-d-Aspartate Receptor with (R)-<sup>11</sup>C-Me-NB1. *J. Nucl. Med.* **2022**, *63*, 936–941. [[CrossRef](#)]
87. Bernard-Gauthier, V.; Bailey, J.J.; Mossine, A.V.; Lindner, S.; Vomacka, L.; Aliaga, A.; Shao, X.; Quesada, C.A.; Sherman, P.; Mahringer, A.; et al. A Kinome-Wide Selective Radiolabeled TrkB/C Inhibitor for in Vitro and in Vivo Neuroimaging: Synthesis, Preclinical Evaluation, and First-in-Human. *J. Med. Chem.* **2017**, *60*, 6897–6910. [[CrossRef](#)]
88. Gallezot, J.-D.; Nabulsi, N.; Henry, S.; Pracitto, R.; Planeta, B.; Ropchan, J.; Lin, S.-F.; Labaree, D.; Kapinos, M.; Shirali, A.; et al. Imaging the Enzyme 11β-Hydroxysteroid Dehydrogenase Type 1 with PET: Evaluation of the Novel Radiotracer <sup>11</sup>C-AS2471907 in Human Brain. *J. Nucl. Med.* **2019**, *60*, 1140–1146. [[CrossRef](#)]
89. Delva, A.; Koole, M.; Serdons, K.; Bormans, G.; Liu, L.; Bard, J.; Khetarpal, V.; Dominguez, C.; Munoz-Sanjuan, I.; Wood, A.; et al. Biodistribution and Dosimetry in Human Healthy Volunteers of the PET Radioligands [<sup>11</sup>C]CHDI-00485180-R and [<sup>11</sup>C]CHDI-00485626, Designed for Quantification of Cerebral Aggregated Mutant Huntingtin. *Eur. J. Nucl. Med. Mol. Imaging* **2022**, *50*, 48–60. [[CrossRef](#)]
90. Johansen, A.; Holm, S.; Dall, B.; Keller, S.; Kristensen, J.L.; Knudsen, G.M.; Hansen, H.D. Human Biodistribution and Radiation Dosimetry of the 5-HT<sub>2A</sub> Receptor Agonist Cimbi-36 Labeled with Carbon-11 in Two Positions. *EJNMMI Res.* **2019**, *9*, 71. [[CrossRef](#)]
91. Coughlin, J.M.; Du, Y.; Lesniak, W.G.; Harrington, C.K.; Brosnan, M.K.; O’Toole, R.; Zandi, A.; Sweeney, S.E.; Abdallah, R.; Wu, Y.; et al. First-in-Human Use of <sup>11</sup>C-CPPC with Positron Emission Tomography for Imaging the Macrophage Colony-Stimulating Factor 1 Receptor. *EJNMMI Res.* **2022**, *12*, 64. [[CrossRef](#)] [[PubMed](#)]
92. Ikawa, M.; Lohith, T.G.; Shrestha, S.; Telu, S.; Zoghbi, S.S.; Castellano, S.; Taliani, S.; Da Settimo, F.; Fujita, M.; Pike, V.W.; et al. <sup>11</sup>C-ER176, a Radioligand for 18-KDa Translocator Protein, Has Adequate Sensitivity to Robustly Image All Three Affinity Genotypes in Human Brain. *J. Nucl. Med.* **2017**, *58*, 320–325. [[CrossRef](#)] [[PubMed](#)]
93. Brier, M. Phase 1 Evaluation of <sup>11</sup>C-CS1P1 to Assess Safety and Dosimetry in Human Participants. *J. Nucl. Med.* **2022**, *64*, 1775–1782. [[CrossRef](#)]
94. Antoni, G.; Lubberink, M.; Sörensen, J.; Lindström, E.; Elgland, M.; Eriksson, O.; Hultström, M.; Frithiof, R.; Wanhainen, A.; Sigfridsson, J.; et al. In Vivo Visualization and Quantification of Neutrophil Elastase in Lungs of COVID-19 Patients—A First-In-Human Positron Emission Tomography Study with <sup>11</sup>C-GW457427. *J. Nucl. Med.* **2022**, *64*, 263974. [[CrossRef](#)]
95. Van Weehaeghe, D.; Koole, M.; Schmidt, M.E.; Deman, S.; Jacobs, A.H.; Souche, E.; Serdons, K.; Sunaert, S.; Bormans, G.; Vandenberghe, W.; et al. [<sup>11</sup>C]JNJ54173717, a Novel P2X<sub>7</sub> Receptor Radioligand as Marker for Neuroinflammation: Human Biodistribution, Dosimetry, Brain Kinetic Modelling and Quantification of Brain P2X<sub>7</sub> Receptors in Patients with Parkinson’s Disease and Healthy Volunteers. *Eur. J. Nucl. Med. Mol. Imaging* **2019**, *46*, 2051–2064. [[CrossRef](#)] [[PubMed](#)]

96. Miyazaki, T.; Nakajima, W.; Hatano, M.; Shibata, Y.; Kuroki, Y.; Arisawa, T.; Serizawa, A.; Sano, A.; Kogami, S.; Yamanoue, T.; et al. Visualization of AMPA Receptors in Living Human Brain with Positron Emission Tomography. *Nat. Med.* **2020**, *26*, 281–288. [[CrossRef](#)]
97. Naganawa, M.; Nabulsi, N.; Henry, S.; Matuskey, D.; Lin, S.-F.; Sliker, L.; Schwarz, A.J.; Kant, N.; Jesudason, C.; Raley, K.; et al. First-in-Human Assessment of <sup>11</sup>C-LSN3172176, an M1 Muscarinic Acetylcholine Receptor PET Radiotracer. *J. Nucl. Med.* **2021**, *62*, 553–560. [[CrossRef](#)]
98. Shrestha, S.; Kim, M.-J.; Eldridge, M.; Lehmann, M.L.; Frankland, M.; Liow, J.-S.; Yu, Z.-X.; Cortes-Salva, M.; Telu, S.; Henter, I.D.; et al. PET Measurement of Cyclooxygenase-2 Using a Novel Radioligand: Upregulation in Primate Neuroinflammation and First-in-Human Study. *J. Neuroinflammation* **2020**, *17*, 140. [[CrossRef](#)]
99. Du, Y.; Coughlin, J.M.; Brosnan, M.K.; Chen, A.; Shinehouse, L.K.; Abdallah, R.; Lodge, M.A.; Mathews, W.B.; Liu, C.; Wu, Y.; et al. PET Imaging of the Cannabinoid Receptor Type 2 in Humans Using [<sup>11</sup>C]MDTC. *Res. Sq.* **2022**. [[CrossRef](#)]
100. Van der Weijden, C.W.J.; Meilof, J.F.; van der Hoorn, A.; Zhu, J.; Wu, C.; Wang, Y.; Willemsen, A.T.M.; Dierckx, R.A.J.O.; Lammertsma, A.A.; de Vries, E.F.J. Quantitative Assessment of Myelin Density Using [<sup>11</sup>C]MeDAS PET in Patients with Multiple Sclerosis: A First-in-Human Study. *Eur. J. Nucl. Med. Mol. Imaging* **2022**, *49*, 3492–3507. [[CrossRef](#)]
101. Kubota, M.; Seki, C.; Kimura, Y.; Takahata, K.; Shimada, H.; Takado, Y.; Matsuoka, K.; Tagai, K.; Sano, Y.; Yamamoto, Y.; et al. A First-in-Human Study of <sup>11</sup>C-MTP38, a Novel PET Ligand for Phosphodiesterase 7. *Eur. J. Nucl. Med. Mol. Imaging* **2021**, *48*, 2846–2855. [[CrossRef](#)] [[PubMed](#)]
102. Ruiz-Bedoya, C.A.; Ordonez, A.A.; Werner, R.A.; Plyku, D.; Klunk, M.H.; Leal, J.; Lesniak, W.G.; Holt, D.P.; Dannals, R.F.; Higuchi, T.; et al. <sup>11</sup>C-PABA as a PET Radiotracer for Functional Renal Imaging: Preclinical and First-in-Human Study. *J. Nucl. Med.* **2020**, *61*, 1665–1671. [[CrossRef](#)] [[PubMed](#)]
103. Sakata, M.; Ishibashi, K.; Imai, M.; Wagatsuma, K.; Ishii, K.; Zhou, X.; de Vries, E.F.J.; Elsinga, P.H.; Ishiwata, K.; Toyohara, J. Initial Evaluation of an Adenosine A<sub>2A</sub> Receptor Ligand, <sup>11</sup>C-Preladenant, in Healthy Human Subjects. *J. Nucl. Med.* **2017**, *58*, 1464–1470. [[CrossRef](#)] [[PubMed](#)]
104. Kim, M.-J.; Lee, J.-H.; Juarez Anaya, F.; Hong, J.; Miller, W.; Telu, S.; Singh, P.; Cortes, M.Y.; Henry, K.; Tye, G.L.; et al. First-in-Human Evaluation of [<sup>11</sup>C]PS13, a Novel PET Radioligand, to Quantify Cyclooxygenase-1 in the Brain. *Eur. J. Nucl. Med. Mol. Imaging* **2020**, *47*, 3143–3151. [[CrossRef](#)] [[PubMed](#)]
105. Tucker, E.W.; Guglieri-Lopez, B.; Ordonez, A.A.; Ritchie, B.; Klunk, M.H.; Sharma, R.; Chang, Y.S.; Sanchez-Bautista, J.; Frey, S.; Lodge, M.A.; et al. Noninvasive <sup>11</sup>C-Rifampin Positron Emission Tomography Reveals Drug Biodistribution in Tuberculous Meningitis. *Sci. Transl. Med.* **2018**, *10*, 145. [[CrossRef](#)]
106. Lohith, T.G.; Tsujikawa, T.; Siméon, F.G.; Veronese, M.; Zoghbi, S.S.; Lyoo, C.H.; Kimura, Y.; Morse, C.L.; Pike, V.W.; Fujita, M.; et al. Comparison of Two PET Radioligands, [<sup>11</sup>C]FPEB and [<sup>11</sup>C]SP203, for Quantification of Metabotropic Glutamate Receptor 5 in Human Brain. *J. Cereb. Blood Flow Metab.* **2017**, *37*, 2458–2470. [[CrossRef](#)]
107. Lee, I.K.; Jacome, D.A.; Cho, J.K.; Tu, V.; Young, A.; Dominguez, T.; Northrup, J.D.; Etersque, J.M.; Lee, H.S.; Ruff, A.; et al. Imaging Sensitive and Drug-Resistant Bacterial Infection with [<sup>11</sup>C]-Trimethoprim. *J. Clin. Investig.* **2022**, *132*, e156679. [[CrossRef](#)]
108. Watanabe, Y.; Mawatari, A.; Aita, K.; Sato, Y.; Wada, Y.; Nakaoka, T.; Onoe, K.; Yamano, E.; Akamatsu, G.; Ohnishi, A.; et al. PET Imaging of <sup>11</sup>C-Labeled Thiamine Tetrahydrofurfuryl Disulfide, Vitamin B1 Derivative: First-in-Human Study. *Biochem. Biophys. Res. Commun.* **2021**, *555*, 7–12. [[CrossRef](#)]
109. Wong, D.F.; Comley, R.A.; Kuwabara, H.; Rosenberg, P.B.; Resnick, S.M.; Ostrowitzki, S.; Vozzi, C.; Boess, F.; Oh, E.; Lyketsos, C.G.; et al. Characterization of 3 Novel Tau Radiopharmaceuticals, <sup>11</sup>C-RO-963, <sup>11</sup>C-RO-643, and <sup>18</sup>F-RO-948, in Healthy Controls and in Alzheimer Subjects. *J. Nucl. Med.* **2018**, *59*, 1869–1876. [[CrossRef](#)]
110. Masdeu, J.C.; Pascual, B.; Fujita, M. Imaging Neuroinflammation in Neurodegenerative Disorders. *J. Nucl. Med.* **2022**, *63*, 45S–52S. [[CrossRef](#)]
111. Chen, Z.; Haider, A.; Chen, J.; Xiao, Z.; Gobbi, L.; Honer, M.; Grether, U.; Arnold, S.E.; Josephson, L.; Liang, S.H. The Repertoire of Small-Molecule PET Probes for Neuroinflammation Imaging: Challenges and Opportunities beyond TSPO. *J. Med. Chem.* **2021**, *64*, 17656–17689. [[CrossRef](#)] [[PubMed](#)]
112. Janssen, B.; Vugts, D.; Windhorst, A.; Mach, R. PET Imaging of Microglial Activation—Beyond Targeting TSPO. *Molecules* **2018**, *23*, 607. [[CrossRef](#)] [[PubMed](#)]
113. Jain, P.; Chaney, A.M.; Carlson, M.L.; Jackson, I.M.; Rao, A.; James, M.L. Neuroinflammation PET Imaging: Current Opinion and Future Directions. *J. Nucl. Med.* **2020**, *61*, 1107–1112. [[CrossRef](#)] [[PubMed](#)]
114. Narayanaswami, V.; Dahl, K.; Bernard-Gauthier, V.; Josephson, L.; Cumming, P.; Vasdev, N. Emerging PET Radiotracers and Targets for Imaging of Neuroinflammation in Neurodegenerative Diseases: Outlook Beyond TSPO. *Mol. Imaging* **2018**, *17*, 1536012118792317. [[CrossRef](#)]

**Disclaimer/Publisher's Note:** The statements, opinions and data contained in all publications are solely those of the individual author(s) and contributor(s) and not of MDPI and/or the editor(s). MDPI and/or the editor(s) disclaim responsibility for any injury to people or property resulting from any ideas, methods, instructions or products referred to in the content.